

6-2012

In vivo Characterization of Deformation Fields in Hypertense Amphibian Hearts Using the Speckle Image Photogrammetry Technique

Mcolisi Dlamini

Union College - Schenectady, NY

Follow this and additional works at: <https://digitalworks.union.edu/theses>



Part of the [Mechanical Engineering Commons](#)

Recommended Citation

Dlamini, Mcolisi, "In vivo Characterization of Deformation Fields in Hypertense Amphibian Hearts Using the Speckle Image Photogrammetry Technique" (2012). *Honors Theses*. 802.

<https://digitalworks.union.edu/theses/802>

This Open Access is brought to you for free and open access by the Student Work at Union | Digital Works. It has been accepted for inclusion in Honors Theses by an authorized administrator of Union | Digital Works. For more information, please contact digitalworks@union.edu.

Department of Mechanical Engineering at Union College

Senior Project Report for the 2011-2012 Academic Year

**IN VIVO CHARACTERIZATION OF DEFORMATION FIELDS IN
HYPERTENSE AMPHIBIAN HEARTS USING THE SPECKLE IMAGE
PHOTOGRAMMETRY TECHNIQUE**

Submitted by:

Mcolisi Dlamini

15 March 2012

Academic Terms

Fall 2011 & Winter 2012

Advised by:

Ronald B. Bucinell, Ph.D., P.E.

ABSTRACT

Author: Mcolisi Dlamini

Advisor: Professor Ronald B. Bucinell (Department of Mechanical Engineering)

***In vivo* Characterization of Deformation Fields in Hypertense Amphibian Hearts Using the Speckle Image Photogrammetry Technique**

Abstract

Hypertension, a major cardiovascular disease, is one of the most prevalent and death causing disease worldwide. In the US, over 70 million adults have high blood pressure, that is, 1 in 3. A prolonged state of hypertension cause damages to the brain cells, the kidneys and can lead to a stroke. This research studies the biomechanical response of amphibian hearts *in vivo* when in hypertensive. A normotensive state is used as the control. Hypertension is induced by injecting a saline fluid directly into the heart ventricle using a syringe. The response of the heart is characterized by monitoring surface deformation fields using the speckle image photogrammetry technique. This is a non-contact optical full field strain technique that uses the ARAMIS photogrammetry software to monitor surface deformations over the entire three dimensional heart over several heart beats. The ARAMIS software is connected to two high speed cameras capable of taking more than 500 frames per second at full field. This technique was successfully used before to characterize myocardial infarction on amphibian hearts. The internal ventricle pressure is measured using a catheter pressure transducer located in the heart. The pressure inside the heart is directly related to the stress on the heart walls which are made of myocardia. During hypertension, the ventricle fluid volume is increased leading to the heart muscles contracting more forcefully. Preliminary results verified this concept with an increase in the deformations of the ventricle from a normotensive state to a hypertensive state. The results obtained showed a displacement increase of 0.18 mm corresponding to 12%. Major strains increased by 6%. The study also investigated whether the ventricle contraction mechanism is a sphere chamber model or a peristaltic tube model. The collected data supports the sphere chamber model. However, more experimentation is required to make these conclusions concrete.

TABLE OF CONTENTS

Description	Page Number
Table of contents	2
Introduction	3
Background	16
Experimental Procedure	19
Results	48
Discussion	54
Conclusion	57
Recommendations	57
References	59
Appendix	61

INTRODUCTION

Hypertension is one of the most prevalent and death causing disease in the category of cardiovascular diseases. Cardiovascular diseases (CVD's) are the world's largest killers. About 17 million people worldwide die from CVD's per year. In 2030 it is projected that CVD's will claim the lives of about 23 million people [1]. Cardiovascular diseases are also known to be the major causes of deaths in the United States. About 82 million Americans have one or more types of CVD's [2]. CVD's are the causes of about 30% of all deaths in the US. In 2006 alone high blood pressure killed over 56,500 people in the United States. About 74.5 million adults in the United States have high blood pressure [2]. The most recent statistics, published in 2012 on hypertension estimate hypertension prevalence to be 27% in the US. 71% of these are aware of their condition and 57% are receiving treatment [3]. The report also claims that there is about 8% undiagnosed hypertension. The National Institute of Health claims that about 1 in 3 Americans have high blood pressure.

Hypertension, commonly referred to as high blood pressure (HBP) is defined as a systolic pressure of at least 140 mm Hg and/or a diastolic pressure of at least 90 mm Hg [5]. In the United States having been told by a physician at least two times that that you have hypertension qualifies as a diagnosis. More generally hypertension is known as the condition when the arterial blood pressure is higher than usual. High forces against arterial walls imply that the heart should pump blood – to the arteries – at a higher pressure to meet volume requirements. During a state of hypertension the heart is the most affected organ in the body and it is also the one that can directly adjust the levels of blood pressure in the blood. The kidneys can alter or cause hypertension by changing the amount of salts in the blood. Their response is delayed leaving the

heart as the only organ responding to short term hypertension. High blood pressure is caused by several factors including stress but it is mainly caused by unknown factors. A prolonged state of hypertension, leads to serious cardiovascular complications and can cause damage to the brain cells, the kidneys and can lead to a stroke.

There are two main kinds of hypertension; primary and secondary. Primary hypertension is the most prevalent type and sometimes referred to as essential hypertension. No direct causes have been identified for this type. On the other hand, secondary hypertension is defined to be caused by an identifiable cause. This hypertension is usually treated by treating the cause. The main strategy for preventing hypertension is practicing good life and dietary habits which include exercise and less alcohol consumption, to name a few. Life style modifications are even recommended for treating hypertension though diuretics and calcium channel blockers are also used when necessary.

A few hypotheses have been developed to explain the pathophysiology of hypertension. However, the mechanisms associated with primary hypertension are still far less understood. Currently scientists know and describe the processes the heart is subjected to during a hypertension but only qualitatively and/or even hypothetically. The goal of this research is to characterize, qualitatively and quantitatively, the heart mechanisms during a hypertension on a bullfrog's heart with the ultimate goal of extrapolating the results to human hearts.

The next paragraphs will introduce the cardiovascular research that has been ongoing at Union College for approximately a decade now. This history will then be followed by an elaborate description of the human heart analog used, the technique for inducing hypertension and lastly the objective of this research will be stated.

History of the Project at Union College

This research is a continuation of the works of at least seven other Union College alumni. These students were mainly from the mechanical engineering department and a few from the biology department. It is also worth noting that this research has been a collaboration with Professor Leo Fleishman, a Biology Professor here at Union, from the very onset up to the present. He has been a huge contributor and a valuable resource especially for the mechanical engineering students who partook in this research. For example, he suggested the use of frog's heart instead of rabbit's heart as an analog for the experiments conducted under this research.

Scott Robinson '03 was the pioneer for this research at Union College. He worked on this research for his senior project in 2003 – 2004. He first worked on rabbit hearts in the summer of 2002 when he was doing an internship with Dr. Glenn Gaudette, at the department of Biomedical engineering at the state University of New York at Stony Brook. At Stony Brook, they were using a single camera and a dissected rabbit heart. Their experiments were conducted *in vitro* using a technique called Computer Aided Speckle Interferometry (CASI). For his senior project, Robinson brought this research to Union College. He switched the analog for the research from rabbit hearts to frog hearts as advised by Professor Fleishman. This enabled experiments to be conducted *in vivo*. He further introduced a 3D technique using Steric Speckle Image Photogrammetry [6]. This new technique used two cameras hence he was able to rid the problem of parallax, which occurs when one is using a single camera. Basically, with a single camera sizes of the object in the field of view could increase either because they are physically increasing or because they are getting closer to the lens. Cameras unlike humans, who have brains, can not differentiate whether the increase in size is due to the object moving closer or

actually getting bigger. The same analogy holds for decreasing in size or moving away from the lens.

Adam Grieco '04 worked on this research for his senior project in 2003 – 2004. He focused on refining the lighting technique. Lighting was causing significant glare and heating the specimen. Significant glare results to low quality images hence it is a serious problem.

Amanda Goodman '07 also contributed to this research, with a focus on refining the speckling technique. She tried many combinations and finally identified titanium dioxide powder and charcoal as the most promising. These substances do not only have to be inert, but also yield a combination or rather a speckling pattern that can be clearly tracked by the photogrammetry system.

Matthew T. Adams '09 and Rachel Fitz '09 pursued this research as well. Adams, in addition, worked on this research over the summer and continued on it for his senior project in 2008 – 2009. One of his many contributions was refining the use of titanium dioxide powder and charcoal. He defined appropriate particle size and the procedure to achieve this particle size. He also explored and refined the use of cool light sources to eliminate specimen heating. Heat from the lights dries the surface of the specimen which will be best kept moist, not only to match conditions inside the animal but also to ensure that the heart continues beating for a longer time period. Most importantly, the surfaces of the frog's heart are kept moist and cool to conserve the *in vivo* conditions of the heart. As a possible solution to the lighting sources, Adams explored the use of polarized lighting. These also reduce glare. He further attempted to integrate a pressure transducer into the heart during measurements. This is essential in the study of hypertension as it give the pressure changes before, during and after the hypertensive state.

Furthermore, Adams developed the technique of using liquid nitrogen to simulate myocardial infarctions. In this technique, liquid nitrogen drops were applied on a specific spot on the heart's ventricle. Liquid nitrogen freezes the myocardia which prevents the muscles from contracting. No oxygen passes through these cells since there is no blood flow, hence the cells underneath suffer hypoxia. This greatly impacts the contraction of the ventricle. But most importantly the lack of oxygen and nutrients to these cells of the heart damages them which induce myocardial infarction. The duo of Adams and Fitz was the first to successfully induce myocardial infarction and collect good data. Fitz, as the biologist, later focused mainly on analyzing the data that was obtained on the biology point of view.

One of the recent contributors to this research is James Maher who pursued his senior project on this research in 2009 – 2010. One of his main focuses was refining the technique of polarizing light to reduce glare.

Leah Pepe '11 a biology major worked on this research for her thesis. Her focus was hypertension which she calls the silent killer. Her objectives were: (1) to find the best model for vertebrate heart: peristaltic tube or compressed sphere chamber model. (2) Study the effects of hypertension on the heart's shape and pumping mechanisms and (3) analyze the distribution of stress on the ventricle whether it is proportionally distributed or not. I was fortunate to work alongside Pepe while doing a practicum on this research. Most of Pepe's objectives were partly adopted for this senior project with the intent of refining the data collecting technique hence increase the accuracy of the data. The data processing method Pepe used indicated the existence of some phenomenon and through this research her findings would be extended and substantiated. Increasing the accuracy of the data will help strengthen and exhaust all possible fallacies regarding the conclusions reached. Figure 1 shows the timeline of this project at Union.

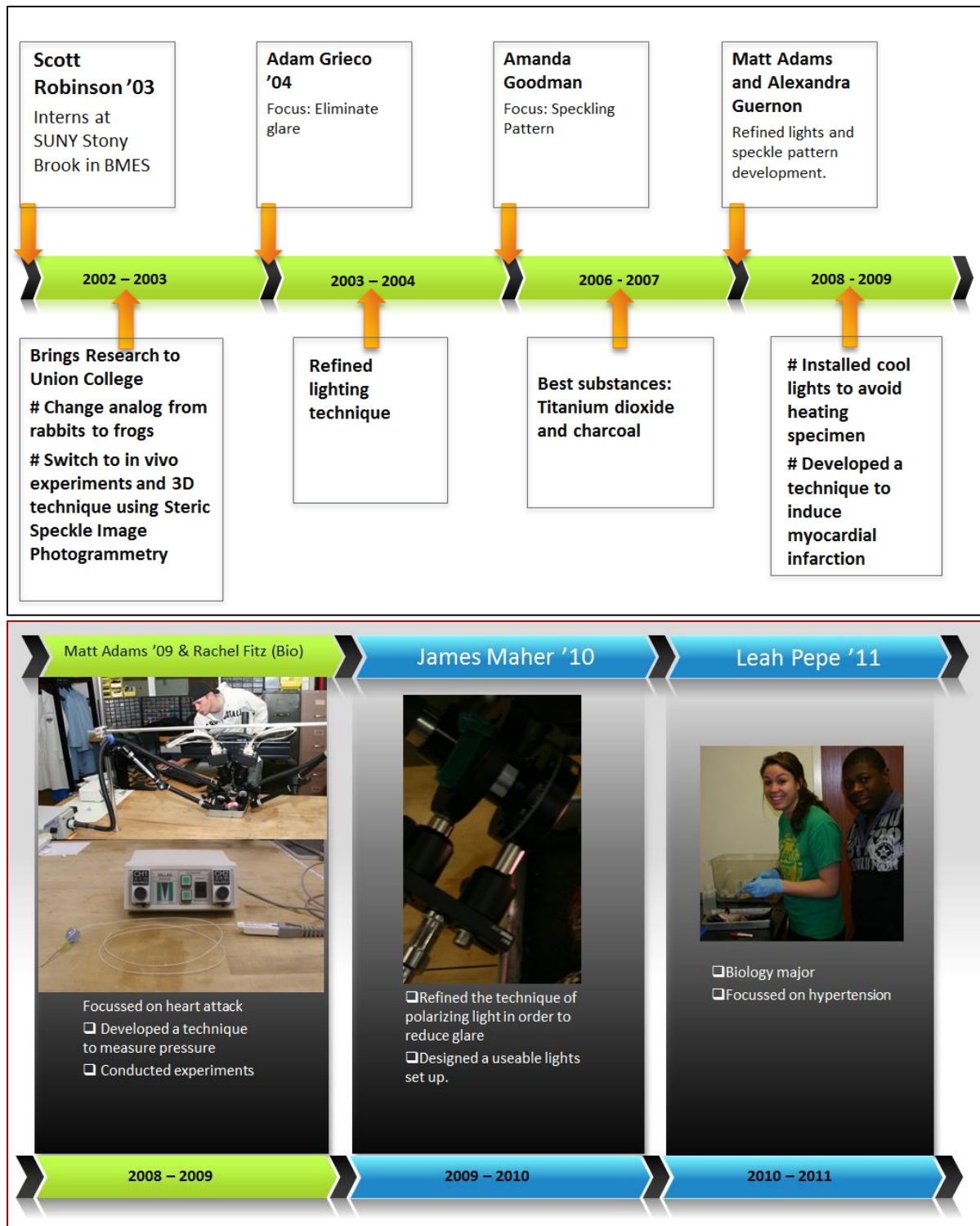


Figure 1: This is the timeline for this research at Union College from Scott Robinson in 2002 to Leah Pepe in 2011.

Tremendous progress was achieved by the previous students who worked on this research. However, several issues that require developments and refinement still remained. One of the techniques that were not fully developed was that of inducing hypertension on the frog heart. Also, the technique for using a pressure transducer in the heart during measurements still required a lot of improvements. The main problem with the pressure transducer was that the catheter needle-tip, which had to be inserted into the heart, was rather large. The problem then is how can this needle be inserted into the heart without damaging the heart tissue? Since a less disruptive technique was not founded, a smaller mikro-tip was the next best alternative. The polarized lights have been tried before but without much success. Therefore, the objective of optimizing the polarized lighting technique to eliminate glare in *in vivo* measurements was explored.

The last student researcher to work on this project, Leah Pepe '11 developed the proof of concept for the contraction models of the heart and the response of the heart to hypertension. The refinement on the data collection technique this research added was using the photogrammetry system to measure deformations on the entire surface of the heart in three dimensions, as opposed to the four points on heart in two dimensional images Pepe used. A speckle pattern is developed on the heart using white titanium dioxide and black charcoal powders. ARAMIS traces this pattern during experiments and computes deformations based on the changes of this pattern. Additionally, the pressure changes inside the frog's heart were to be measured using a catheter transducer. Due to time constraints, this was never done but a calibration was performed for a much thinner needle recently acquired. This would give a better understanding of the pressure changes before, during and right after hypertension.

The Frog's Heart

Bullfrog hearts were chosen as the best specimen for this research. Though different from human hearts, to a greater extent the two are very similar. Figure 2 shows a labeled ventral view of the frog's heart.

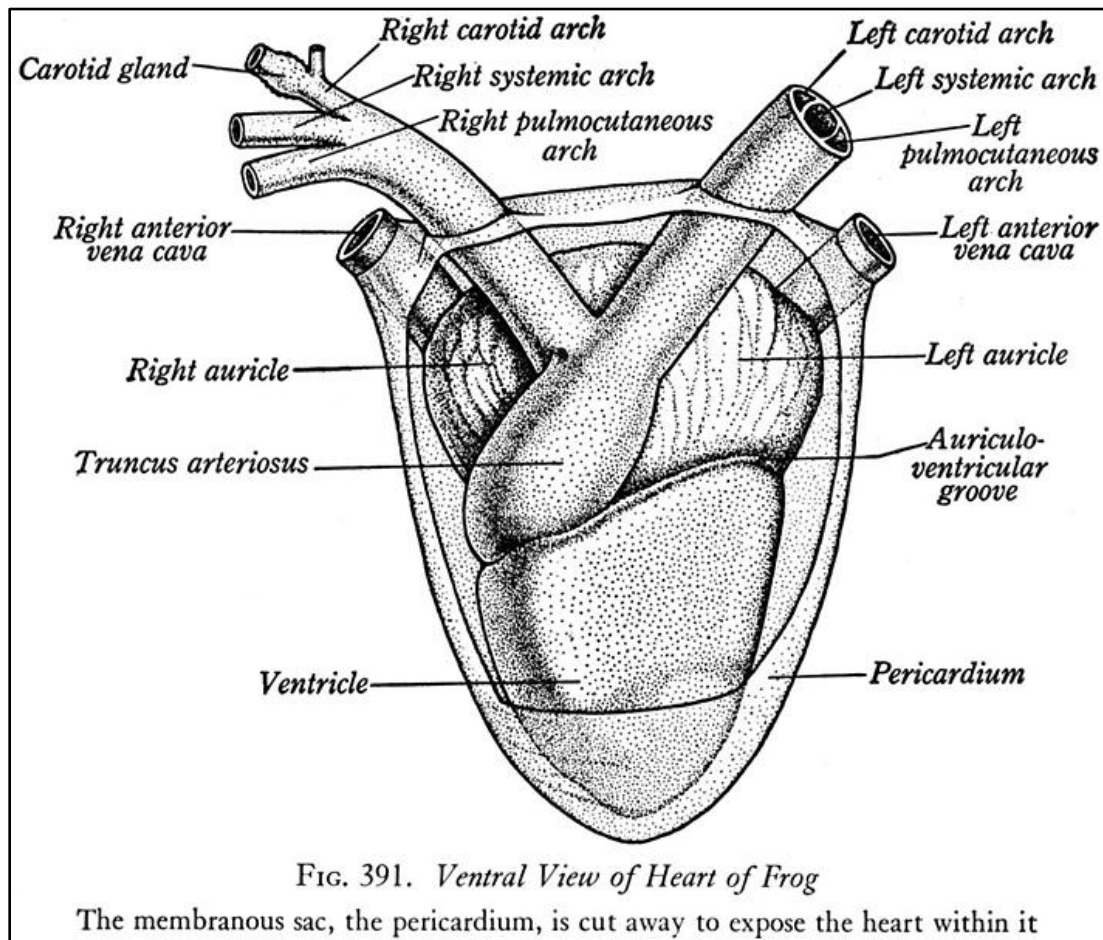


Figure 2: The anatomy of a frog heart showing the single ventricle and the two atria. The muscles of this heart are the same as those on a human heart. [9]

A common misconception is that since the frog's heart has one ventricle, the oxygenated blood from the lungs and the deoxygenated blood from the rest of the body mix in the ventricle. In the frog heart, the oxygenated and deoxygenated blood is separated even though the ventricle is undivided [10]. As a result of this 'separation' the oxygenated blood from the lungs is guided

and directed to the rest of the body via the systemic arch. On the other hand, deoxygenated blood from the body is guided and directed to the lungs via the pulmocutaneous arch. The spiral folding within the *conus arteriosus* of the heart aids this separation. The contraction of the ventricle pumps the blood to the lung circulation which once 'full' then blood flows to the systemic circulation. The amount of blood for each circulation is regulated by the resistance each arch offers. Immediately following a breath, the resistance to blood flow through the lung is low and blood flow is high; between breaths, resistance gradually increases and is associated with a fall in blood flow [10, Page 483]. Therefore, it can be inferred that when the frog is not breathing at all which is the case during the experiment, less blood or almost no blood is pumped to the lungs at all.

The major reason the heart has one ventricle is because there is no need for a second one. The blood is pumped out of the heart at the same pressure. Amphibians also generally require less oxygen. For example they can survive without breathing and when this happens no blood flows to the lungs. This is the other reason the frog heart continues to beat after the frog has been pithed.

Frogs have very low metabolism rates hence the low amounts of oxygen required by their bodies. In addition to low metabolism, they can respire through their skin which complements for breathing especially after they have been pithed. Skin respiration is impossible for mammals including human beings. The circulatory system of the frogs then continues working 'normally' after pithing mainly because of these two reasons, low metabolism and skin respiration.

The Human Heart

Figure 3 shows the human heart with a clear view of the two ventricles and the two atria.

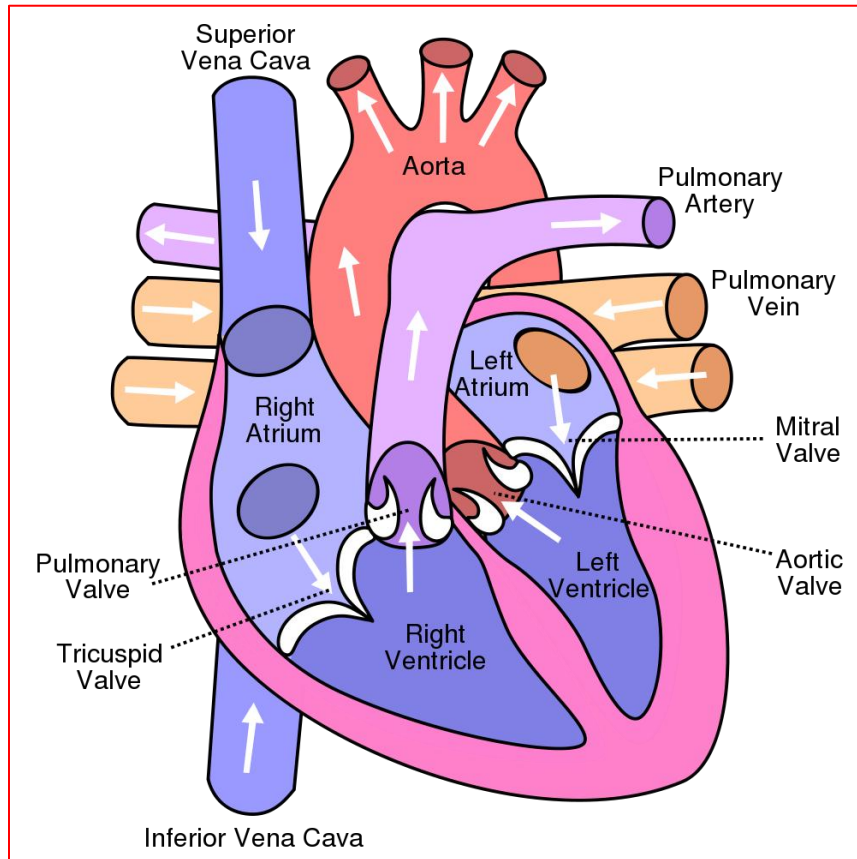


Figure 3: A labeled diagram of the human heart. The human heart has two ventricles as opposed to a single ventricle on the frog's heart. [11]

As mentioned earlier, the human heart has two ventricles, which is the main difference between the frog's heart and the human heart. It is worth noting that the two ventricles are a result of evolution responding to the need of high oxygen concentration difference in the two circulatory systems and their pressure differences. The human circulatory system has two major systems: the pulmonary circulation and the systemic circulation. In systemic circulation the blood travels from the heart to the head and the rest of the body except the lungs. The left ventricle is the part of the heart that produces the pressure required to pump the blood in this

circulation. The aortic arc helps distribute the blood from the left ventricle to all directions. The blood from the left ventricle is nutrient and oxygen rich hence it has to go to all parts of the body to satisfy the cell's oxygen and nutrients requirement. The pulmonary circulation pumps blood from the heart to the lungs. The blood returns to the heart oxygenated. The right ventricle is responsible for the pressure required for this cycle. Due to proximity of the two organs, less pressure is required for the pulmonary circulation compared to the systemic circulation. It is impossible for one ventricle to pump blood at different pressures, hence the two ventricles. Since the left ventricle pumps at a higher pressure, it developed a thicker layer of myocardia, the heart muscle cells as compared to the right ventricle.

A frog heart is most suitable for this study because it allows for measurements to be done *in vivo*. The frog heart continues pumping blood for over an hour after the frog has been pithed. During this period, enough data can be acquired for a normotensive condition and a hypertension state. The types of cells on the human heart and frog heart are the same and contract in a similar fashion. This will be essential when the results of this research are interpolated to human hearts. The fact that amphibian hearts continue to beat after the nervous system has been destroyed was the chief reason for choosing frogs.

Inducing Hypertension

Hypertension was induced by injecting a salt water solution into the ventricle of the heart. "Hypertension can be represented by increased fluid volume (Guyton 1992). With increased extracellular fluid volume, blood volume increases. With an increased blood volume there is an increase in average circulatory filling pressure (Guyton 1992). This pressure increases the amount of

venous blood returned to the heart forcing the heart to pump even harder to move the blood through the pulmonary circuit and then the systemic circuit (Guyton 1992).” [5]

The increase of the volume of the heart forces the ventricle to contract more forcefully. The length of each contraction is lowered too. When this happens, hypertension has been induced. The pressure inside the heart would be measured to give the evidence of hypertension. The description given above is for a human heart. The same approach was used for the frog heart. The only difference is that there is one ventricle responsible for both circulations.

Objective of this research project

There were two main objectives for this research. The first objective was to characterize the deformations of a heart during a simulated hypertension. The second objective was to investigate the most suitable breathing model for the heart. A bull frog heart, *Rana catesbeiana*, was used as the analog to a human heart. Hypertension, in general terms, is a condition of high blood pressure (HBP). As mentioned already hypertension is defined as a systolic pressure of at least 140 mm Hg and/or a diastolic pressure of at least 90 mm Hg [5]. The heart responds to hypertension by pumping a larger volume of blood more forcefully to quickly return to an ambient state, also known as a normotensive state. The biomechanical response of the heart was studied by observing the changes due to hypertension in the strain magnitude and distribution on the heart. The dangers of hypertension to humans – damage to kidneys, brain cells and strokes – are the motivation behind understanding the natural response of the heart to hypertension. Once this has been qualitatively and quantitatively understood, the ultimate goal would be to be able to enforce this response in hearts that can no longer naturally restore pressure changes to normal levels.

The hypothesized contraction models for the heart are a sphere chamber model and a peristaltic tube model. Animal's breathing models are described generally by one of these two models. Peristaltic tube implies that the heart contracts like a tube where the muscles do not all contract synchronically but the contraction wave moves from one end to the other. A sphere chamber model is when the entire heart walls contract at the same time and pressure is generated by decreasing sphere volume. The volume of the heart was also monitored during the change from ambient to a hypertensive state.

In the next chapter, the background of hypertension and what research scientists have and are currently pursuing is discussed. The technique and equipment used to conduct experiments is discussed in the experimental procedure section of this document. This section provides a detail explanation of the system and technique used to capture the data before and during hypertension. The data was then processed to yield the deformations on the heart which suggest the breathing mechanism as well as the heart's response to hypertension. A discussion section is included which leads to the conclusion and recommendations suggested by the author.

BACKGROUND

In this section the focus will be on past and ongoing hypertension research. Hypertension is not a new condition hence its research dates back. However, the techniques employed in the study of hypertension have evolved over years. The ARAMIS Photogrammetry technique used for this research is very recent and is not widely used in this research area.

Hypertension research dates back to the early twentieth century – when scientists could actually measure blood pressure. It was then that Physicians began associating high blood pressure with risks for heart failure, stroke and kidney failure [9]. In the 1940's research was mainly focused on lowering blood pressure thorough the use of case studies. The outcome in 1958 was the development of a diuretic called chlorothiazide. These are still in use today although recent innovations have been implemented, for instance, calcium channel blockers (CCBs). Since the late 1980's several recommendations have been made on how to prevent hypertension development.

Nowadays, scientists understand the complications associated with hypertension. Research has partly shifted to understanding prehypertension. The danger with hypertension is the lack of obvious symptoms. A majority of researchers now focus on relating hypertension with other diseases like diabetes. The likelihood of having hypertension based on race is also under investigation. For example, recent studies have claimed that African Americans are more likely to have hypertension.

In the future, hypertension will be investigating the use of peoples genomes and prepare antihypertensive therapies ahead of time for them. Genetic variants studies and programs like SPRINT: Systolic Blood Pressure Intervention Trial, focusing on intensive techniques for

lowering systolic blood pressure seems to be establishing the basis for future work in this area. Technological advancements now and in the future, allow for a better understanding of already investigated concepts. It is these technologies that encourage researchers to venture into research like this one, with the hope to upgrade the understanding of breathing models of the heart and its natural response to upsets like hypertension; with the hope of coming up with new prevention and treatment methods.

Scott Robinson, in the summer of 2002, worked as an intern at SUNY Stony Brooke with Professor Glenn Gaudette studying full field deformation on the heart of rabbit hearts. The studies were conducted in vitro and they were only using one camera which presents the issue of parallax. There studies were not very successful. Professor Glenn Gaudette, before he transferred from SUNNY Stony Brooke to WPI, performed extensive research measuring deformations of the surface of the heart using CASI: Computer Aided Speckle Interferometry. In his published paper, he discusses that CASI results were in agreement with sonomicrometry. CASI requires speckling patterns which for these experiments silicon carbide particles with a diameter of 40 micrometers were used. Robinson then brought this research at Union.

At Union College cardiovascular disease research has been going on for about ten years now. Matthew Adams, in 2007 - 2008 researched under the topic “*IN VIVO* measurement of strain field gradients in an amphibian heart after artificially induced myocardial infarction.” Adams for this research used the ARAMIS photogrammetry software and applied the speckling photogrammetry technique. Liquid nitrogen was applied on the surface of interest on the frog heart using a metal probe. This froze the heart cells resulting to hypoxia and nutrients to these cells and cells below. This induced a state of myocardial infarction or simply called a heart

attack. Pressure changes were monitored using a pressure transducing catheter which was synchronized with the ARAMIS Software. Adams observed that during the heart attack there is a reduction in the Z displacement of the heart and an increase of both the major and minor strains for the amphibian heart. The experiments conducted are similar to those performed under the current research except that this time hypertension is induced as opposed to myocardial infarction.

Leah Pepe '11 extended this research to hypertension. Her results suffice as a demonstration of the phenomenon. This research's main goal is to refine the data collected, by measuring deformation fields on entire heart surface instead of point displacements. Based on the new data, the pre-conclusions will either be reaffirmed or adjusted.

EXPERIMENTAL PROCEDURE

In this section the apparatus and the procedure used to conduct the experiments for this research will be discussed in depth. First, the apparatus themselves will be introduced and then their preparations before experiments which include processes like calibration will be discussed. This discussion will be done per component and then the whole system put together will be discussed, mainly to give the experimental procedure for a real experiment. Components discussed in depth are the ARAMIS Photogrammetry system and the pressure catheter transducer. Techniques will include the pithing technique which is used to prepare the frog for experiments, the speckling technique, how to eliminate glare and the use of polarized lighting to reduce specimen heating.

The ARAMIS Photogrammetry System

The figure below shows the ARAMIS Gom v.6.3 as it would appear during a real experiment. This system is situated in the Mechanics Lab located in Butterfield at Union College. It has been in use for about 10 years now and its application varies but its pivotal use is to study fast occurring deformations. ARAMIS is a commercial software made by GOM Optical Measuring techniques (GOM mbH, Braunschweig, Germany) and distributed to US customers by Trillion Optical Test Systems. This is a non-contact optical full field strain technique providing 3D displacements, surface strain fields and values for major and minor strains to mention a few. The technique uses a speckling pattern from which it generates coordinates that it traces throughout the course of an experiment. The coordinates form the center of facets which

are made of pixels. ARAMIS translates the movement of these pixels into displacement vectors. It is from these displacement vectors that strain vectors are computed. The ARAMIS software is combined with high speed photography which yields hundreds of images from which the software computes the strain calculations. The high speed cameras allow for the study of fast rate deformation experiments. For these experiments a catheter pressure transducer was connected to monitor the pressure changes inside the frog's ventricle. The catheter transducer is connected to the ARAMIS software and the two are synchronized for a better understanding of the changes the heart undergoes during a hypertension.

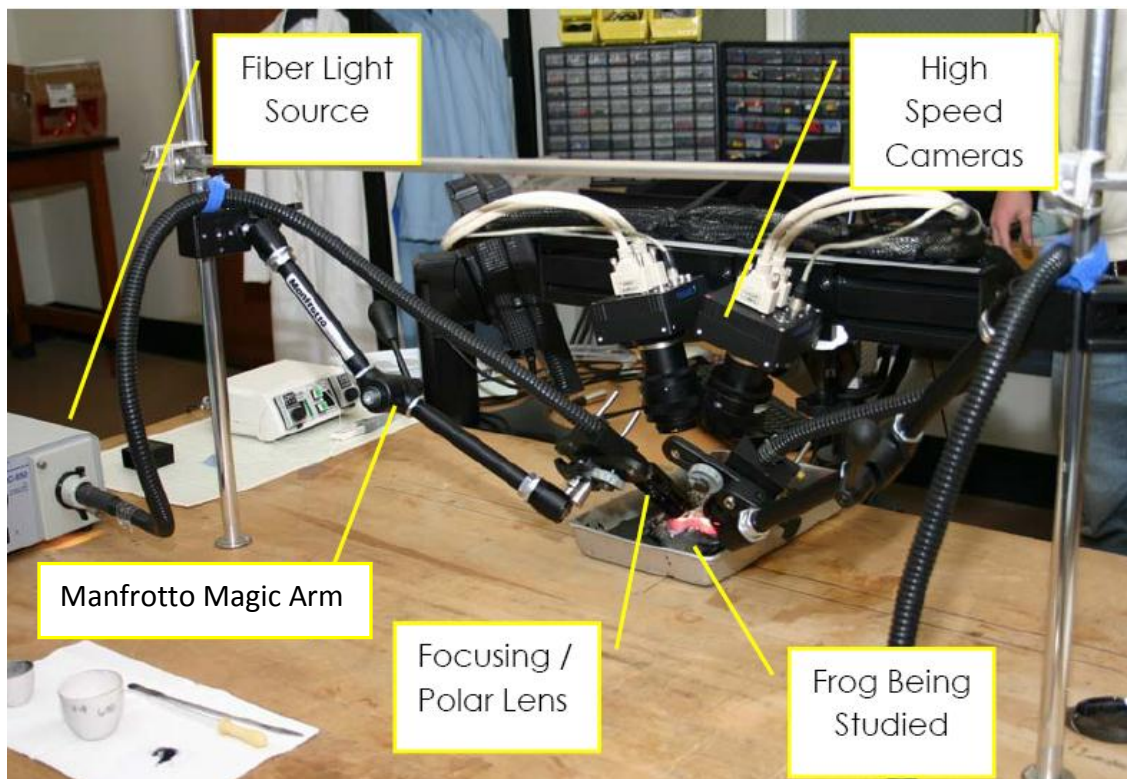


Figure 4: The ARAMIS Photogrammetry System set up during an experiment. [Courtesy of Matthew Adams]

Figure 4 is an image of the system during an experiment taken by Matthew Adams when he was studying myocardial infarctions using the ARAMIS photogrammetry system in 2008. A similar set up for hypertension was used. The two cameras shown are high speed cameras that can take images at a rate of 500 frames per second at full field. When the field of view is compromised, they can operate at a rate of 8 000 frames per second. The rate of these cameras allow for measurements of very fast occurring movements to be measured. The system uses two high speed cameras (Basler A504k, Basler Vision Technologies, Made in Germany), both focusing on the same image at a time, resulting to three dimensional images and deformations.

The light sources used are fiber optics lights. They are suitable for this system because they provide very intense lights as required but most importantly, they are a cool lighting system. Cool lights are preferred for the frog hearts since they prevent heating and drying the surface of the heart. The manfrotto magic arms are used to position the lights closer to the specimen and to move the lights around if necessary.

ARAMIS Calibration

Before every experiment the ARAMIS Photogrammetry System needs to be calibrated for the desired field of view and depth. Different calibration cubes are used for different field of views. Calibrating the system basically gives the system the unit measurements for the six degrees of freedom which are the three dimensions like the x, y and z directions and the angles with respect to the x, y and z axis. However, this process maybe cumbersome unless one is given a starting point. The starting points that were used for this system were created over the summer of 2011 during my summer research. The frog heart is about 10 mm by 10 mm hence for the

calibration process; the 12 x 15 mm calibration cube was used. This calibration cube is provided in the ARAMIS software package. The starting points created are more of a catalogue that when used properly will give the best or close to calibration results as possible. Appendix A shows the catalogue just for the 12 x 15 mm cube which is shown in figure 5 below.

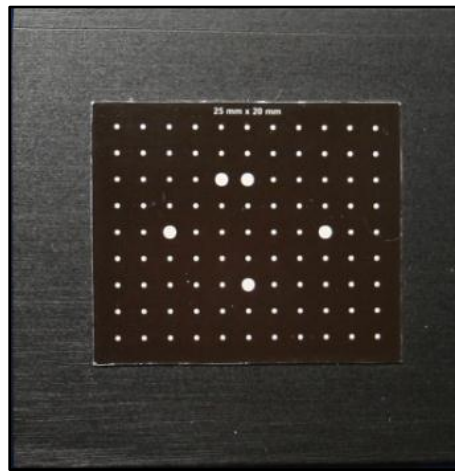


Figure 5: This is the calibration cube that was used to calibrate the ARAMIS system before every experiment.

Appendix A gives the extensions suitable for the calibration cube chosen, the distance between the two cameras, the distance of cameras from the target, and the camera angle. A range of calibration cubes can be used but the choice is guided by the size of the specimen and the deformations expected. The camera extensions mainly affect the size of the image in the field of view. The extensions that were empirically determined to be the best choice for the 12 x 15 mm cube were 35 mm extensions. The distance of the cameras from the target and between each other is directly related to the angle between the two cameras. Of course this assumes that the two cameras are focused on the same image which is a requirement for ARAMIS. It is also necessary to leave enough room between the specimen and the cameras to ensure that the specimen does not touch the cameras during deformation.

One of the dimensions that is very hard to get from ARAMIS is the depth. Therefore, our calibration set ups were optimized for this depth. During the process it was observed that a camera angle between 30° and 34° gave the most depth and a smaller calibration deviation as anticipated. This camera angle was obtained when a small distance between the cameras was used. Generally, this would be a distance of 120 mm to 130 mm. Notice the small range which highlights that good calibration results are only achieved within small parameter ranges.

Depth for this system is solely dependent on the angles of the two cameras. A small angle will present the issue of parallax. This is usually the problem when making observations using a single camera. A single camera does not have depth perception just like one eye. A single camera does not differentiate between an increasing image and an image that is getting closer to the camera itself. In both cases the image will appear to be increasing. The use of two cameras takes care of this possible error.

Fiber Optic Lights

As aforementioned, a cool lighting system is used in the lab mainly to avoid heating the surfaces of the frog heart and at the same time provide very high intensity lights. High intensity lights are a necessity mainly because the system takes hundreds of images in a second. The source for this light is shown in the figure below. This is a Fiber-Lite, DC 50, DC regulated illuminator manufactured by Dolan Jenner Industries.



Figure 6: The fiber lights source providing cool lights used during an experiment.

Using polarized lights: Polarization filters

At the end of the fiber lights are linear polarizing filters. These were obtained from Edmund Industrial Optics. Two light sources are used resulting to two filters on opposite side of the specimen as shown in figure 4. These filters should allow the same amount of energy for the left and right camera. To make sure the two cameras both receive the same amount of energy, first set one filter to zero. Then adjust the other filter until the energy in the two images shown on the computer screen match. The false color option under the view section is chosen to best match the two images. This technique is described in depth below.

Previously, the filters were connected to the end of the lights using a very rudimentary style. Over the summer of 2011, a brass piece was designed and fabricated to securely connect the filters to the lights. The brass piece connects to the piece with the filters using screws. The front of the fiber optics lights then screws to this piece is held securely in place. See figure 7

below. The polarization technique is mainly setting up the polarized filters and using ARAMIS to compare left and right images.

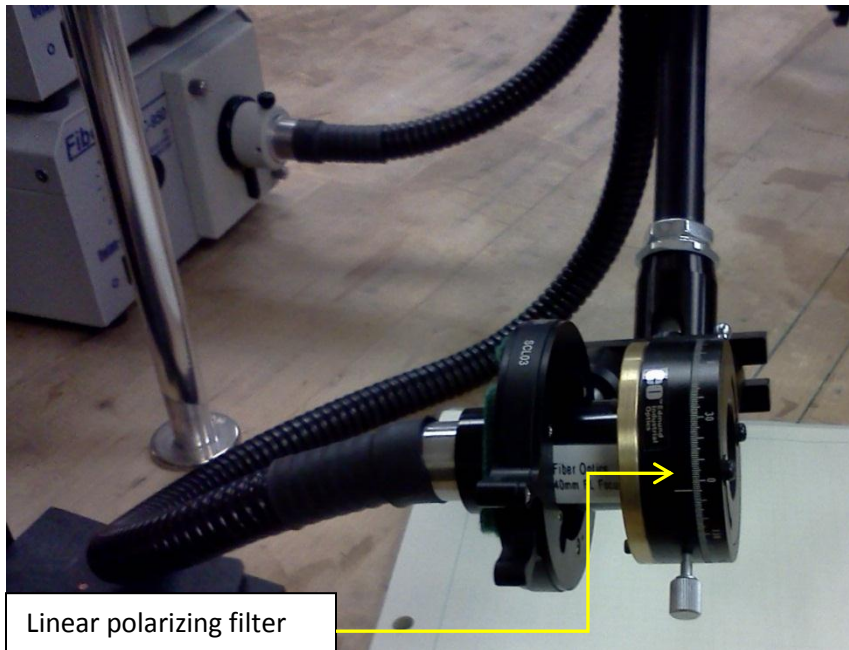


Figure 7: Polarization filter at end of lights holder.

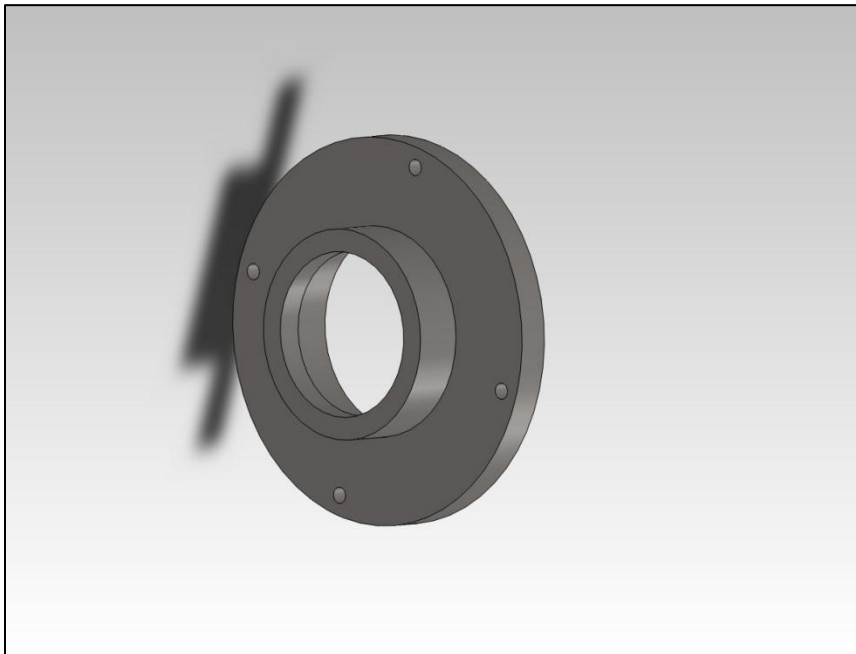


Figure 8: The brass piece designed to hold lights in place as shown in figure 7.

Polarization Technique – Optimization for Glare

The polarization technique is used to optimize for glare while allowing the most light into the cameras. The essential target is to reduce glare and simultaneously increase the light intensity reaching the specimen. Therefore, optimization is performed for these two indirectly related factors. Additionally, this technique attempts to ensure that both cameras receive the same amount of light. The following steps are a simple guide for the polarization technique.

1. Focus both cameras. This could be right before calibrating the system. Once the distance between the cameras has been fixed, then there exists a certain distance between the cameras and specimen (or calibration cube) with the utmost focus. This is determined by moving the cameras vertically and observing both the left and right images. After focusing the cameras the angles of the cameras can then be changed to center the calibration cube.
2. Note that the lights are at their optimum when they hit the cube at an angle of at least 60°. It is important that the lights shown in figure 7 are positioned correctly.
3. Adjust filters on cameras to rid of glare. Rotating the filters on the cameras changes the amount of glare on the image. These should be turned until the least glare remains on image. This is performed on both the right and left images.
4. Then adjust one filter on lights to get the most light and minimum glare (or until you think it is good enough.)
5. This step refines step 4. The goal is to make sure that the same amount of energy reaches both left and right cameras. Switch view mode under visualizations from overexposed or original to false color. While looking at the left image and right image, adjust the other filter until colors on both images match.

6. Switch visualization mode to overexposed or original. The system should be ready to be calibrated now.

Camera Filters

In an attempt to reduce glare, filters were added at the end of the cameras. These are B+W High Performance Filter, 435 5XX 75269, Top-Polarization: Linear. Adjusting the two filters, on the two cameras, rids the glare on the images. It is important to eliminate glare to produce high quality images that ARAMIS will process to output the deformations.

Unfortunately, these filters decrease the amount of light energy entering into the cameras resulting to a demand of more lights.

MEASURING PRESSURE

The pressure this research measures is that of the ventricle of the frog. Pressure is given by the following equation.

$$P = \frac{dF_n}{dA} \quad [1]$$

Where F_n is the force and A is the area where the force is applied. Notice that pressure and stress have the same units of Pa (SI). A catheter pressure transducer is used for this measurement. This stress being measured is the force the blood exerts onto the force of the heart walls. Increasing the volume of blood in the ventricle, which is the basis of volume based hypertension, increases the pressure inside the heart, leading to more stress on heart walls.

Pressure Transducer

A pressure transducer is an instrument used to measure pressure gage mainly of fluids like air and water. Figure 9 below shows the pressure transducer used for this research.

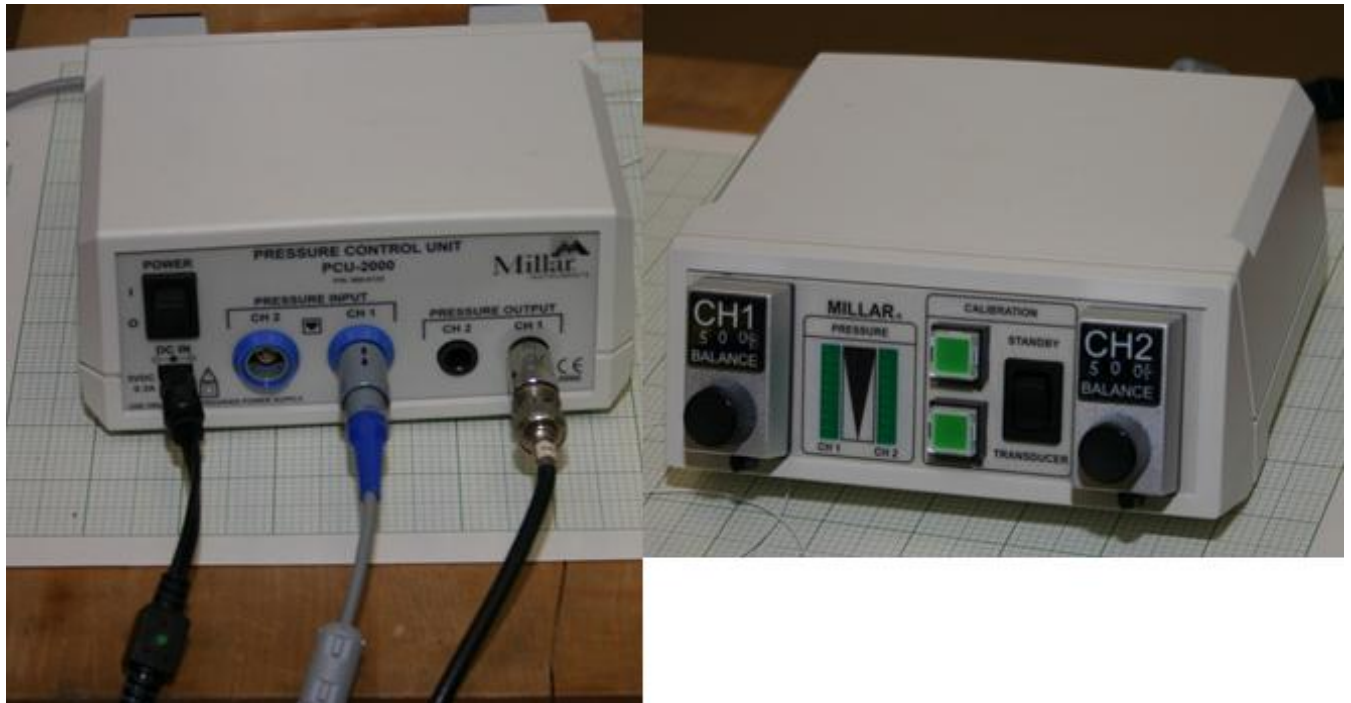


Figure 9: The pressure transducer from Millar Instruments used to measure pressure inside the heart. On the left is the back of transducer showing the connections to power, catheter and multi-meter. On the right is the front of the pressure transducer.

A PCU – 2000 pressure transducer from Millar Instruments is used to measure the pressure changes in the frog’s heart. Pressure changes are recorded in voltages and transformed to pressure using a calibration equation. The pressure transducer is used in conjunction with a catheter transducer discussed below.

Catheter Transducer

A catheter transducer is an instrument used to measure pressure changes. It connects to the pressure transducer. The catheter transducer currently in the lab is the SPR-524 from Millar Instruments. The important component of the catheter is the Mikro-Tip. This tip is the sensor analogous to a pitot probe except that the pitot probe is for measuring fluid flow velocity. Millar Mikro-Tip pressure catheters provide an ideal solution for measuring highly accurate pressures, whether arterial and ventricular blood pressures.¹

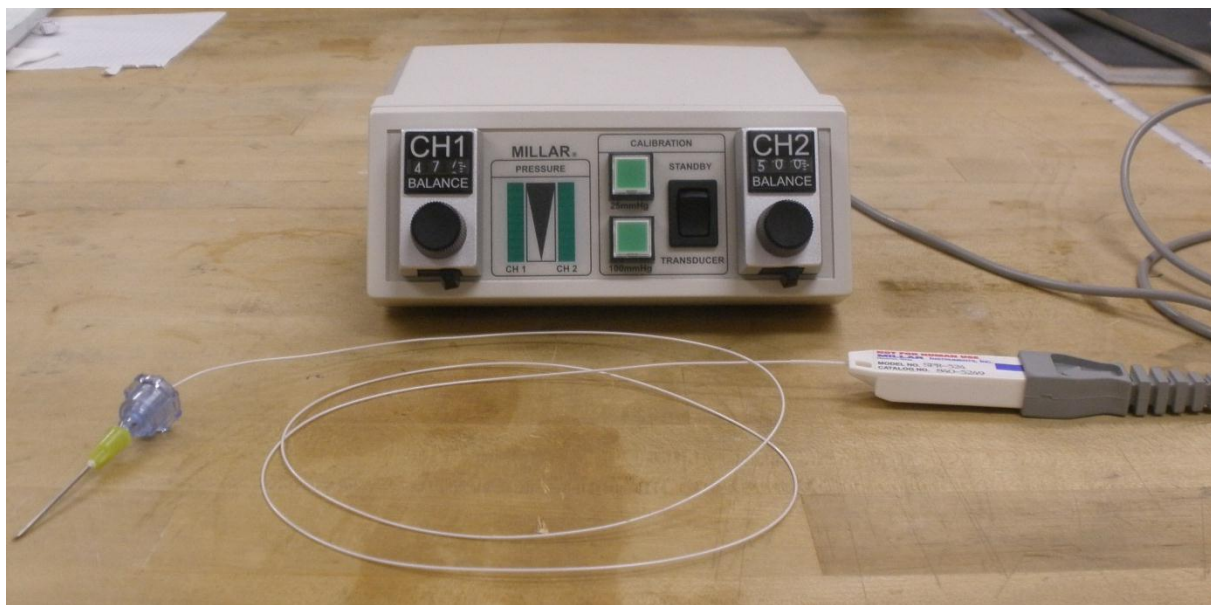


Figure 10: A catheter transducer in front of the pressure transducer. The two are connected.

In normal use, the Mikro-Tip is inserted or placed at the location where the researcher wants to measure the pressure changes. Figure 11 below is an example of how pressure catheters are normally used.

¹ Millar Instruments. Retrieved 8/05/2011. <http://millar.com/products/research/pressure>

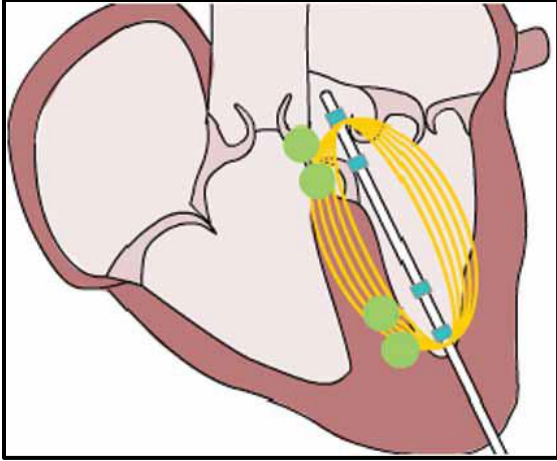


Figure 11: Notice that the catheter is inserted into the catheter. This image was obtained from Millar Instruments research resources. [14]

This implies that for our experiments the Mikro-Tip should be inside the ventricle of the heart. Having considered inserting the Mikro-Tip inside the heart by possibly first poking the heart with a needle and then pushing the tip inside, the final decision was against this. Inserting the Mikro-Tip will definitely cause more damages to the muscles of the heart thereby interfering with the measurements. Alternatively a needle was connected to the end of the blue case with the Mikro-Tip. This needle is then inserted into the heart and it is the only part that goes into the ventricle. Figure 12 shows how this procedure was performed.

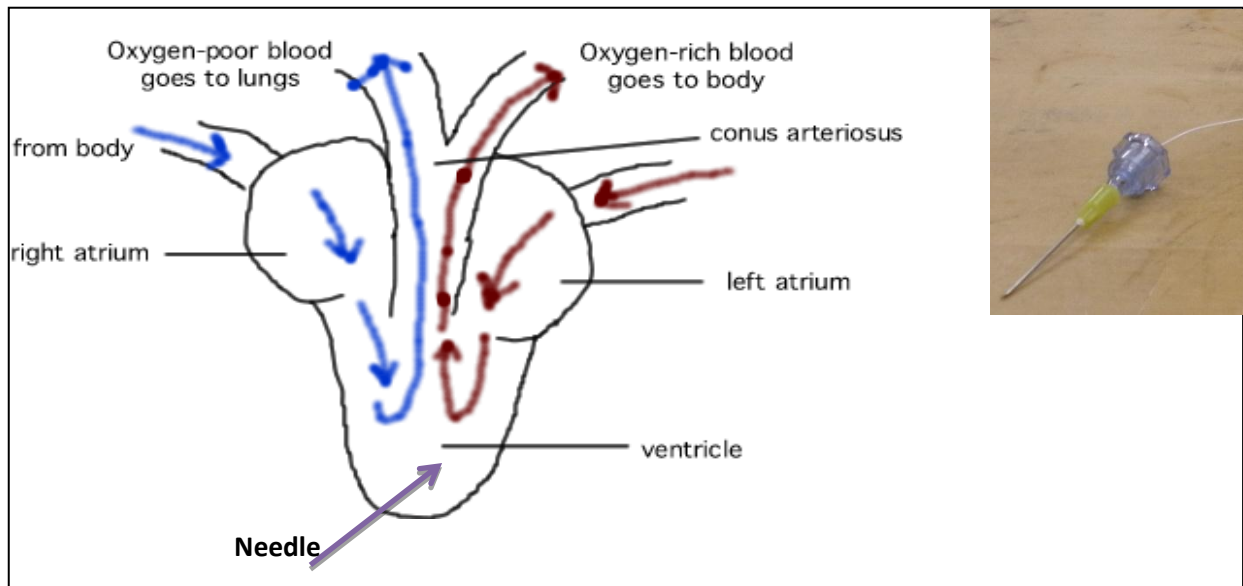


Figure 12: The needle inserted into the frog's ventricle². The needle is further connected to the catheter transducer. Insert (top right) is the actual needle connected to Mikro-Tip.

Needles

The needles used for this research were Kendall Monojet Hypodermic needles shown in figure 13 below. These needles are Kendall Monojet Polypropylene Hub Hypodermic Needles 30GA $\frac{3}{4}$ A 0.3mm 19.0mm, REF 8881 which were bought from TYCO. As mentioned above, the needle is the only part of the pressure measuring system that is inserted into the ventricle of the frog's heart. Therefore, the needle of choice is one that will cause as minimal damage to the myocardium as possible. Simultaneously, the needle should cause less pressure head loss as possible. In the next section, an investigation of the effect of the needle on the pressure readings recorded by the catheter is presented.

² Original image was obtained from the biologycorner.com.



Figure 13: The needles used in the lab. On the left is a 19 Gauge needle and on the right is a 30 Gauge needle. (Courtesy of James Maher)

First, let's introduce the calibration technique used for the pressure transducer and catheter. The same technique will be employed to evaluate the differences of pressures between the 19 gauge needle and the 30 gauge needle.

Pressure Transducer and Catheter Calibration

Deionized water is used to find pressure changes in terms of voltages at depths of known pressures. Figure 14 shows the set up for the pressure calibration.

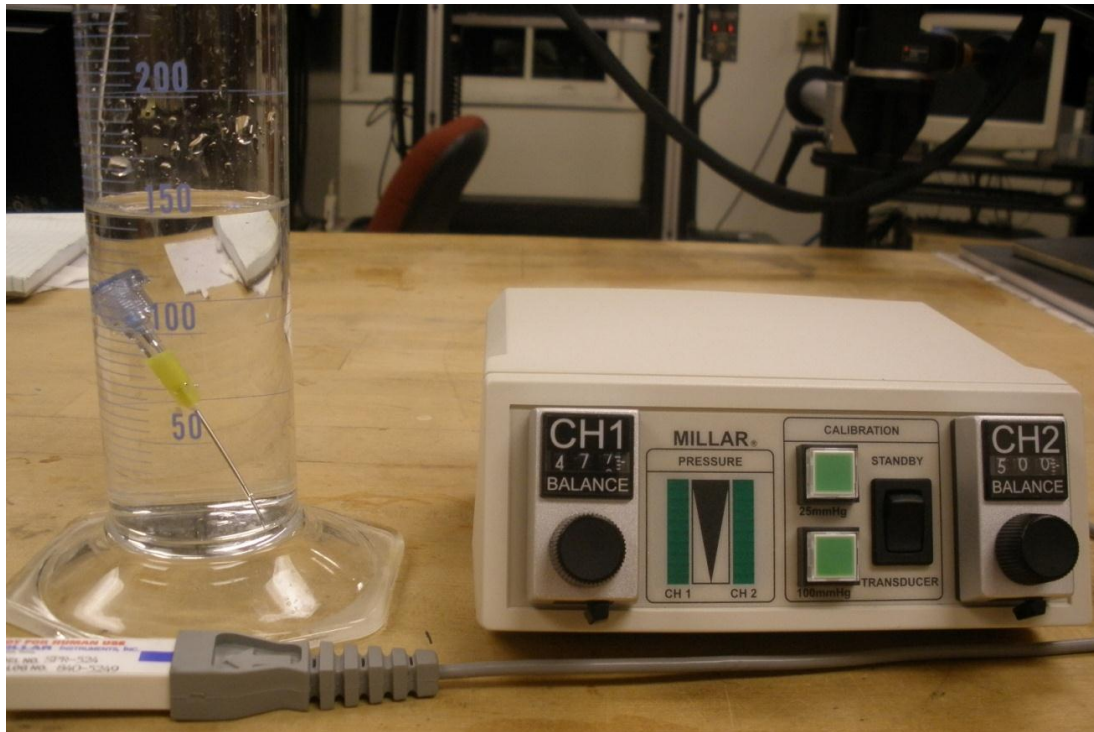


Figure 14: The calibration set up for the catheter transducer.

Materials required

A measuring cylinder or beaker containing de-ionized water is used. It is best if this cylinder has markings for the depth of the water from a known water level which corresponds to zero depth. A voltmeter is required to measure the voltages. ARAMIS can also be used to measure the voltage as it will be the case during a real experiment. The pressure transducer should be connected to the catheter transducer and all components that need power be connected to a power source.

For our calibration, a graduated cylinder was filled with water to the 500 ml mark. Since the cylinder only has markings corresponding to water volume, the heights of these marks were measured hence used for the depth as shown in table 1 first and second column.

Procedure for measuring pressure

The catheter is then put into the water at a known depth and the voltage is measured and recorded. When the needle is connected, the tip of the needle has to correspond to the depth.

Concentric depths are recommended. The table below shows an example of data collected during a calibration.

Table 1: The calibration data for 30 G needle using de-ionized water.

Water Level (mL mark)			Voltage Changes (mV)			Pressure (Pa)	
	Depth (mm)	Δh (mm)	1st Trial	2nd Trial	3rd Trial	Average (mV)	Difference (mV)
450	27.5	27.5	14.2	14.6	14.4	14.40	
400	55	27.5	16.8	18.8	17.8	17.80	3.40
350	82.5	27.5	39.3	41.3	40.6	40.40	22.60
300	110	27.5	58.8	61.8	60.8	60.47	20.07
250	138	28	79.6	81.5	80.8	80.63	20.17
200	165.8	27.8	99.1	99.8	100.5	99.80	19.17
150	193.5	27.7	119.1	120.4	120.8	120.10	20.30
	Average	27.64				-	19.93
	STDEV	0.20				-	1.28

The measurement of the voltage at each depth was repeated three times to reduce experimental errors incurred from the voltage and depth measurements. The average is then calculated and used for further calculations. Thereafter, the voltage difference is computed and averaged. Pressure head loss is given by the equation,

$$\text{Pressure Head Loss} = \rho * g * \Delta h \quad [2]$$

where ρ is the density of water = $1000 \frac{kg}{m^3}$, g is the force of gravity on earth = $9.81 \frac{m}{s^2}$ and Δh is the difference in height. It was also expected that using a smaller needle will increase the head losses incurred. Figure 15 shows the voltages of the 19 gage, 30 gage and no needle. The voltage is directly related to the pressure changes hence for this plot the voltage was used for comparison purposes.

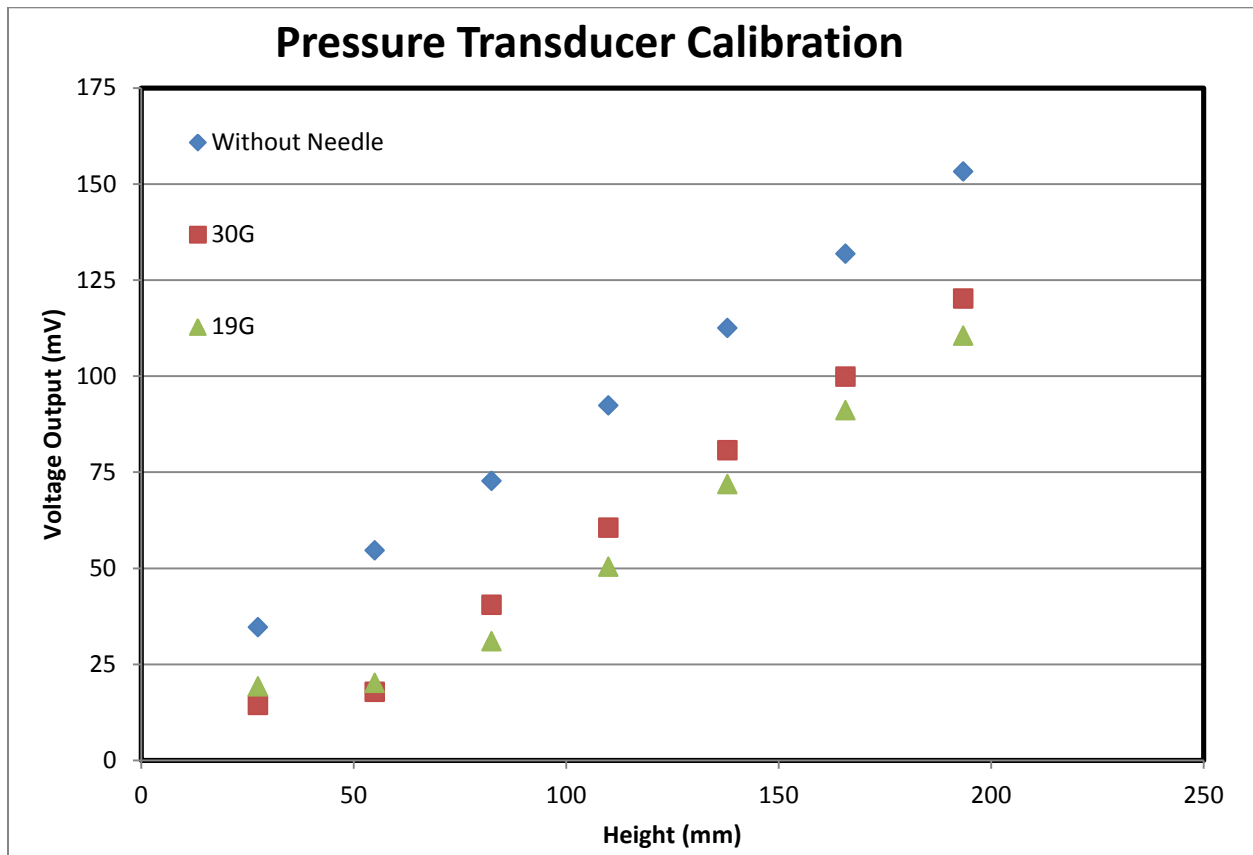


Figure 15: Comparing the voltage changes of the three catheter cases namely; 1) without needle 2) 30 gauge needle and 3) 19 gauge needle.

The differences in voltages at a specific depth correspond to the amount of pressure loss. Surprisingly, the 30G needle has more pressure loss compared to the 19G. The 19G needle is

twice the length of the 30G needle. Assuming that this is the main and only cause of the differences then the following analysis makes sense. Consider equation 2 again which is.

$$\text{Pressure Head Loss} = \rho * g * \Delta h \quad [2]$$

The first two variables would be the same except for the height. Since the 19G needle is twice the length of the 30G needle (height is equivalent to length during calibration) then the pressures should have a 2:1 ratio. 30G is $\frac{3}{4}$ inches long and 19G is 1.5 inches long. However, that is not the case. The reason behind this is the difference in diameters of the two needles. The 19G needle has a nominal inner diameter of 0.686 mm and the 30G has a nominal inner diameter of 0.159 mm.³

Figure 15 above also shows the plot for the voltage when no needle is connected to the mikro-tip. This would be the best choice to use but it is also important to note that of significance to this research are the pressure changes. Additionally, pressure losses will be accounted for in pressure calibration equation which is discussed in detail below.

Pressure Calibration equation

This is the equation that relates the voltage changes being measured to the pressure changes of interest. The pressure inside the cylinder can also be calculated using equation 2.

$$\text{Pressure gauge} = \rho g \Delta h \quad [2]$$

Δh is the depth and is the variable in this equation. This equation gives the pressure gauge at each known depth. Then, the calibration equation relates the voltage changes to pressure changes. The average of pressure changes corresponding to the average voltage changes gives this relationship. Table 2 shows data that was used for this calculation.

³ From <http://www.encyclo.co.uk/define/Needle%20gauge%20comparison%20chart> retrieved 08/21/2011.

Table 2: Pressure and voltage changes measured while calibrating the catheter transducer.

Depth (mm)	Δh (mm)	Average (V)	Difference (V)	Head Loss	Head Loss changes (Pa)	Pressure per voltage (Pa/V)
27.5	27.5	14.40		269.78	269.78	
55	27.5	17.80	3.40	539.55	269.78	79345.59
82.5	27.5	40.40	22.60	809.33	269.78	11936.95
110	27.5	60.47	20.07	1079.10	269.78	13443.94
138	28	80.63	20.17	1353.78	274.68	13620.50
165.8	27.8	99.80	19.17	1626.50	272.72	14228.77
193.5	27.7	120.10	20.30	1898.24	271.74	13386.06
Average	27.64		19.93		271.41	13669.81
STDEV	0.20		1.28		2.03	385.74

Based on table 4, it was concluded that $1 \text{ Voltage} = 13.7 \text{ kPa}$ for the case when the Mikro-Tip is attached to a 30 G x 3/4" needle. Specifically it is;

$$1 \text{ V} = 13.67 \pm 0.4 \text{ kPa}$$

Figure 16 below shows the relationship between the voltage and pressure changes at different depths.

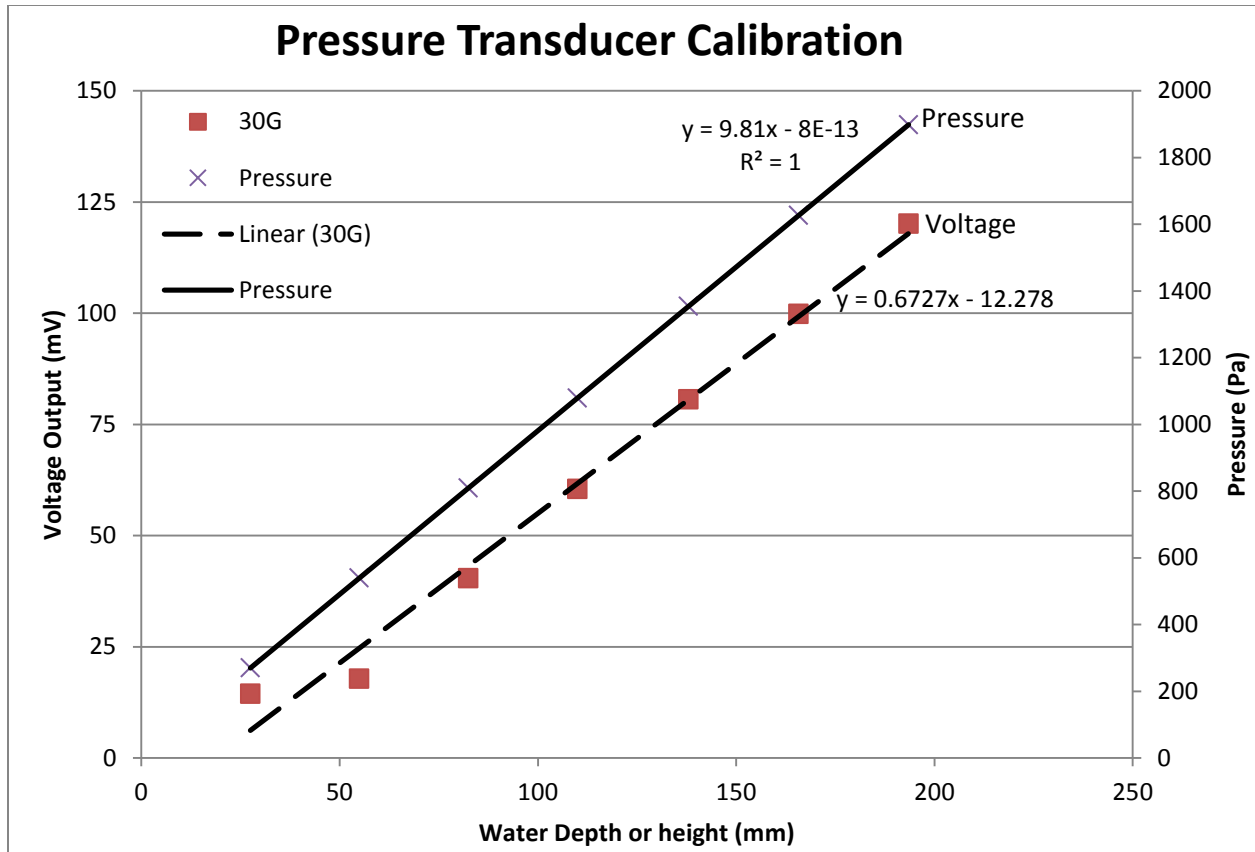


Figure 16: The graphs for voltage and pressure with respect to the depth of the de-ionized water. Appendix C shows all the data and more images used for these computations.

Amphibians Used

The specimen for the three experiments conducted was a marine toad, *bufo marinus* and two bull frogs, *Rana Catesbeiana*. Marine toads are very similar to bull frogs. They were ordered by the biology and taken care of by the same department before the experiments were conducted. The *bufo marinus* are an invasive species that is very dangerous. They multiply very fast and uncontrollably. They have poison compartments next to their necks which kill animals that eat them. In Australia, these toads were introduced as a form of pest control but this turned catastrophic. The *bufo marinus* are being killed daily just because of the danger they pose to other animals. Other strategies to get rid of them are in developmental stages. Bull frogs are also an invasive species.

Frog Preparation

The frog used for this research was prepared for the experiment following the animal research protocols. The frog was taken care of by the biology department of Union College which has people trained on this task. An attempt was made to use the frogs as soon as they got here. Below is a discussion of the frog preparation before, during and after the experiments.

Figure 17 shows an image of a bull frog.



Figure 17: The frog before experiments. This is a bull frog *Rana Catesbeianus*, which is an invasive species. These frogs are rather large and also the poisonous pocket to the right of the eye. [18]

Before the experiment the frog has to be in a state of serene; that is a relaxed or less active state, not traumatized. This is a requirement to ensure a normotensive state of the heart before hypertension is induced during the experiments. To ensure this condition the frog is cooled. It is then pithed to destroy the nervous system. Only trained individuals are allowed to perform the pithing process. Professor Leo Fleishman, co-advisor to this project, is certified to

perform this action. Pithing is described as a technique used to immobilize animals to be used for research. This involves pushing a rod, a pithing rod, through the soft spot at the back of the frog's head, the cranium. Once the rod is pushed into the brains it is shaken from side to side or wiggled around to destroy the brain. After which the rod is inserted down the spinal cord to destroy it too. Once the nervous system has been rendered insensitive, then the frog is ready for dissection. It was assumed that this process happens so fast that the circulatory system remains undisturbed.

Pithing in the past was used as slaughtering technique to kill animals in a manner that was considered humane. This is because the animals do not suffer terrible and prolonged pain; off course with the nervous system destroyed the animal cannot feel anything. Additionally, there is no loss of blood or blood spills in the process. The technique was favored for animals suffering from terrible diseases. In research pithing is used to allow for *in vivo* experiments, like observing the heart as in our case. The frog continues breathing since its breathing is not controlled by the nervous system. The circulatory system continues operating normal for at least half an hour in the case of frogs.

The frog was dissected by Professor Fleishman following the common dissection procedure. The frog was dissected by cutting the midline all the way to its neck on the stomach side. A lateral cut was made on top of the chest and below the abdomen. Figure 18 shows the cuts that were made on the frog during dissection.

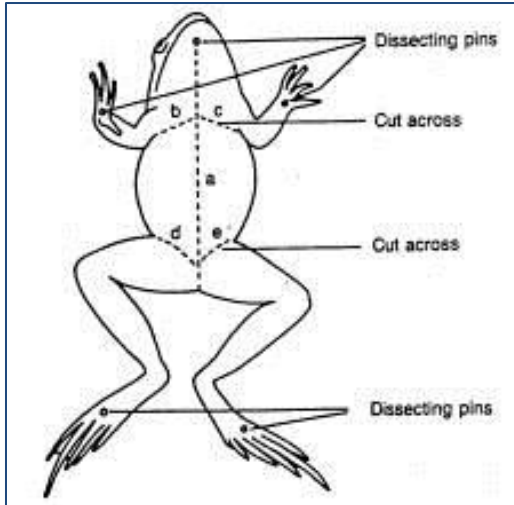


Figure 18: The cuts made on the frog during the dissection process. [19]

After dissecting the frog, it was opened to expose the heart. Figure 19 below shows the dissected frog.

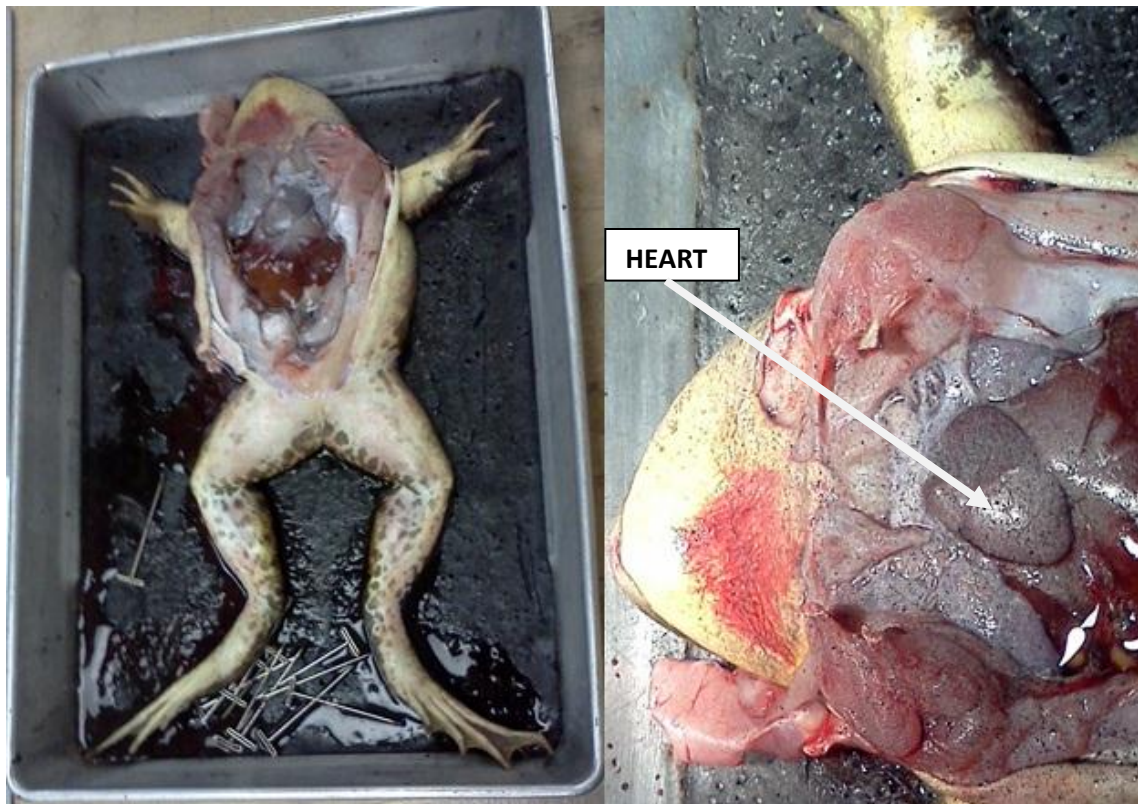


Figure 19: The dissected frog with the heart exposed, speckled and ready for experiments.

Speckling Technique

This technique is an essential component of the ARAMIS photogrammetry technique. Without a proper speckled pattern on the surface of the specimen, no deformations can be computed. The speckling pattern is generated using two contrasting colors preferably black and white. Typical substances or chemicals used are spray paints. For ARAMIS generally, a white spray paint is used for the background and then the black paint is sprayed faintly on top to create the two color contrasts required. Figure 20 shows two examples of a speckle pattern.

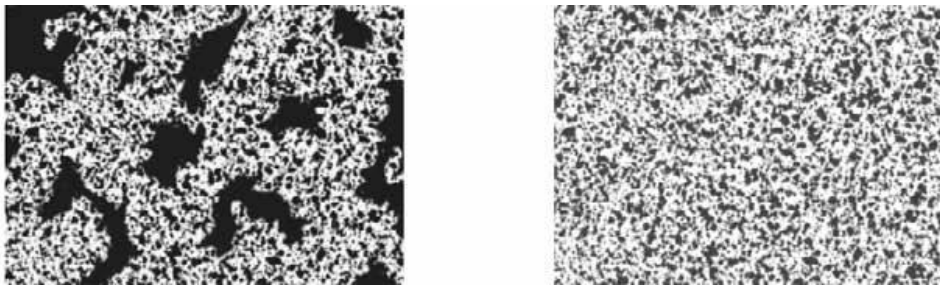


Figure 20: An example of a good high contrast stochastic pattern on the right versus a poor speckling pattern on the left. These images were obtained from the ARAMIS manual.

Unfortunately, for our specimen, the frog's heart, spray paints cannot be used to generate the speckling pattern because the chemicals in these substances react with the surface of the heart. The ideal chemical substances are those that are innate and still present a high color contrast. Amanda Goodman, who worked on the cardiovascular research in 2007 focused on refining the speckling pattern. Goodman concluded that titanium dioxide and charcoal powders provide the best combination for a speckling pattern. These substances are still in use and the most preferred. Adams in 2008 refined this technique and went as far as figuring out the appropriate particle sizes for the titanium dioxide and the charcoal.

The next issue that these substances presented was their application onto the surface of the specimen. Since these substances are powders, they cannot be sprayed onto the heart but

gentle blown onto the surface to try and evenly distribute them over the entire surface. The titanium dioxide is applied first then the charcoal is sparsely and evenly blown on top of the white titanium dioxide layer. Achieving a good high contrast stochastic pattern is almost impossible. A lot of practice went into developing and mastering this technique. Tofu was used for practicing since it closely resembles the frog heart, especially when cut into the heart's shape. Additionally, tofu lasts for a reasonable amount of time allowing for more practice time. Figure 21 and figure 22 shows one of the best speckling patterns developed on tofu.

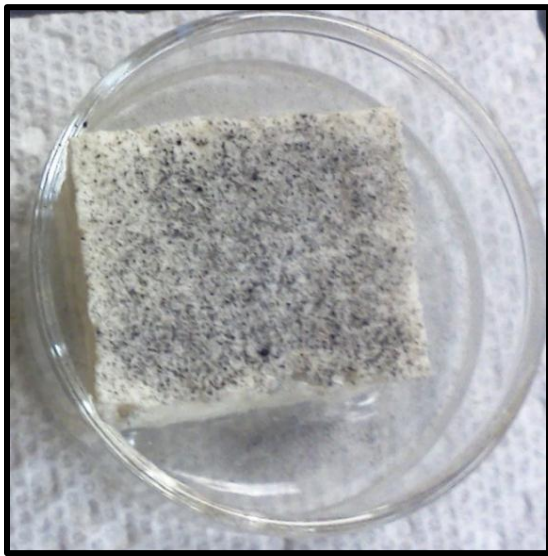


Figure 21: This is an image of speckled tofu ready to be tested for the quality of the speckling pattern on it.

The development of a speckling pattern technique was much harder than expected. More time was spent practicing this technique repeatedly until mastered. It is important to be able to speckle the frog's heart as quickly as possible and as best as possible. Note that the heart will not be stationary during the process, as the frog will be breathing, which makes the process even harder.

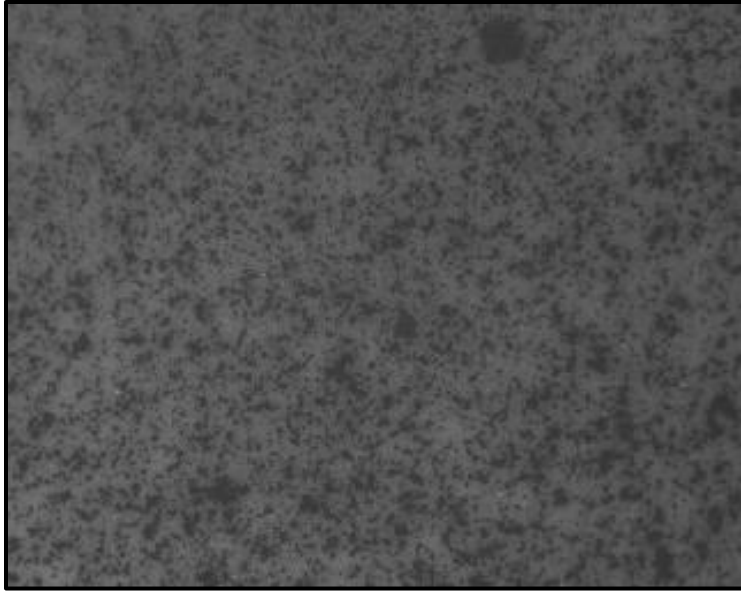


Figure 22: An example of a good speckling pattern on tofu as seen in ARAMIS.

The goal of this extensive practice was to assure that during a real experiment, the pattern can be developed quickly and perfectly. As this was solely a manual process, repetition was necessary for consistency. Heart models would be the ideal practice specimen but in their absence, tofu was the next best option.

To test if the speckling on the tofu was good, strain computation was performed on a few images. To ensure similarity to the frog the tofu was poked to yield movements in the x, y and z directions. The images were taken using the simple mode. For the real experiments a trigger list was used. Figure 23 below shows an image of the tofu with the starting point, the facet field and grid.

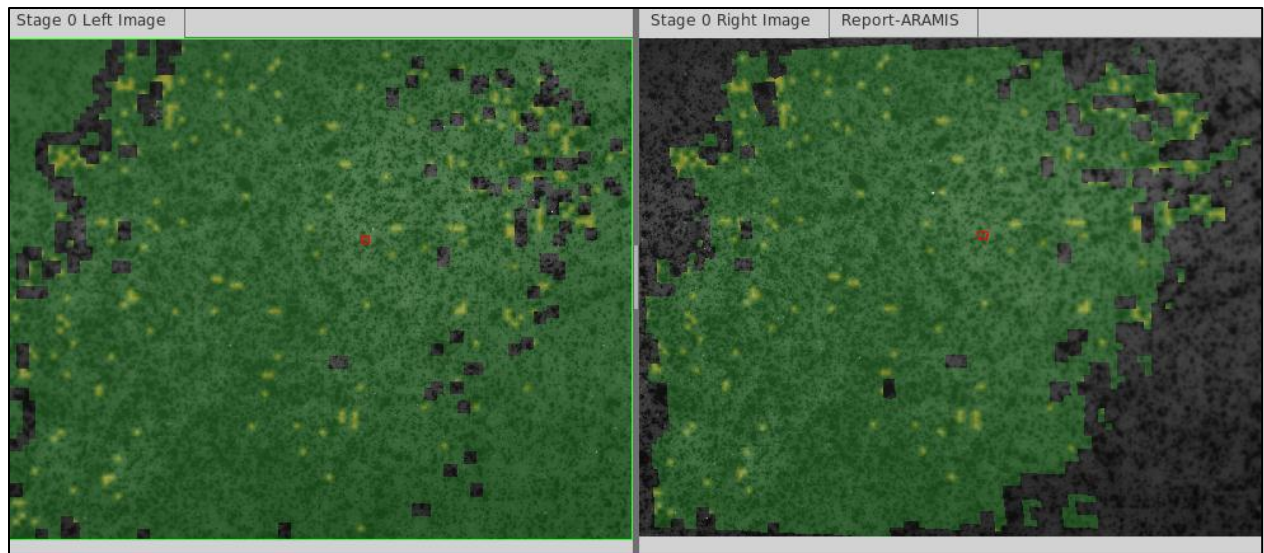


Figure 23: An example of the facet fields developed during the tofu practice for speckling. The sections without facet fields were either out of focus or most probably not speckled well. The yellow colors indicate that the system calibration was not perfect.

Speckling Powders Preparation

White titanium dioxide (TiO_2) powder and black charcoal were used to develop the speckling pattern on the frog's heart. However, the particles needed were much finer than the ones purchased. Therefore, to make small particles, the original charcoal particles were grinded down in a crucible for about 30 minutes. Small amounts were grinded at a time to ensure that all the particles were crushed thoroughly. The titanium dioxide particles were grinded for about five minutes. The prepared powders were then kept in a dehumidifier to make sure that they do not clump while blowing them over the heart during speckling. This also helped to reduce glare in the images and the speckling development successful.

Data Collection and Processing

In the previous paragraphs the whole system and procedures were described. The specimen and materials preparation were also discussed. Data was collected after the frog has been dissected and its heart speckled. Data is collected by taking images of the heart at two different states; normotensive and hypertensive states. The data is stored in the Linux computer that runs the ARAMIS photogrammetry system.

Data processing begins by defining a starting point in all the images. The starting point has to be a facet grid that is recognizable in all the stages. For this experiment it was defined using a semi-automated procedure where it was manually selected for the first image and based on that selection, the starting point was selected automatically for the rest of the images by the program. Once a starting point has been successfully selected, ARAMIS was used to compute the deformations and strains on the data. Reports were then created to summarize the data for a specific variable picked by the user. Generally the reports created were multi-staged and either Z displacement or major strains. Image series reports were also created and these can be obtained by contacting the author.

Experiment 1: Report

The first frog experiment was conducted on the 20th of February 2012. For this experiment a big toad was used as the specimen; scientifically known as a *bufo marinus*, very similar to the bull frog. Data was not successfully collected during this particular experiment due to a few existing issues surrounding the technique used. However, this experiment helped in refining the technique and better prepare for the second experiment. Without this experiment it

would have been impossible to predict what constraints exist on the polarization and speckling techniques. For example, during this experiment it was noted that more light is required to be able to take images at a shorter shutter time. The shutter time used for this experiment was about 100 milliseconds, much longer than required by the fast beating frog heart. The longer shutter time yielded a lot of blur on the images captured. Secondly, it was observed that the specimen has to be perfectly focused to get good images. Developing the speckling pattern on the frog heart, while it is beating, is also more challenging than one would expect.

After this experiment, it was decided that the filters on the cameras need to be removed to increase the amount of light. The tradeoff was the increase in glare on the images, but rather have glare than no data at all. Additionally, halogen lights were added to be used as back up lights in case, more intense lights were needed.

The next section provides the data and calculated results of this research. Some modifications into the set up described in the experimental procedure section were made at times to accommodate for new arising issues. These will be mentioned and explanations for their use provided. The rest of this report will then evaluate the results and make conclusions and recommendations based on the results.

RESULTS

Three experiments were conducted during this research. No usable data was obtained from the first experiment but with the enlightenment obtained in this experiment, the techniques used in this experimental procedure were refined leading to somewhat successful experiments thereafter. It is important to note that experiments that involve the use of animals like this one cannot just be conducted anyhow, but one should be ready to get the most information from every life sacrificed. Consequently, a lot of the time was invested in researching and preparing for the experiments than invested on testing and debugging experimental techniques.

The ARAMIS photogrammetry system was calibrated before every experiment. A calibration deviation less than 0.04 pixels, as the target, was met. After the calibration, the system is ready to take images. The frog was pithed and dissected by Professor Leo Fleishman. Next, a speckling pattern was developed using titanium dioxide and charcoal powders. Images of the frog heart breathing under normal conditions were taken. This is the normotensive or ambient state. Hypertension was induced by injecting the heart with a saline fluid, and images were taken quickly to capture the period of hypertension. Only short term hypertension was induced. The speckling pattern was not always perfect so at times the heart was speckled and cleaned and re-speckled several times. To ensure regular physiological contraction for the heart, a Ringer's solution was sprinkled on the heart in-between speckling patterns.

For the second experiment, a bull frog was used as the specimen. Due to its big size a 23x18 mm cube was used to calibrate the system as opposed to the 15x12 mm that is generally used. The following trigger list was used. A trigger list makes it easy to capture images using

ARAMIS. The trigger list was started at the instant when the frog heart was relaxed – just before the next contraction cycle.

```
#  
# Triggerlist created by GOM-Triggerlist Tool 1.0-2  
#  
## Version: Tom v6.0.2-0  
#  
  
## Element: Fast  
ID=00 n=-1 Hi=1 Lo=0 fgD=1 R=0 T=2 Stop=8 Save=1  
FAST r=100 n=500
```

Figure 24: This image shows the trigger list that was used during the experiments.

The following figures and table summarize the results collected in this research. The first results are for the normotensive state, followed by the hypertensive state and lastly a comparison between the two states. More figures showing these results are attached in appendix D. Videos were also created for the displacements and strains computed using ARAMIS photogrammetry system. These can be viewed by contacting the author.

Experiment 2: Results

Figure 24 and figure 25 show a normal breathing heart – normotensive state. Figure 24 shows the displacement of the frog heart. Notice that the plot on the right is very similar to pressure plots for a normal beating heart. Figures 26 and 27 show results from the hypertensive state.

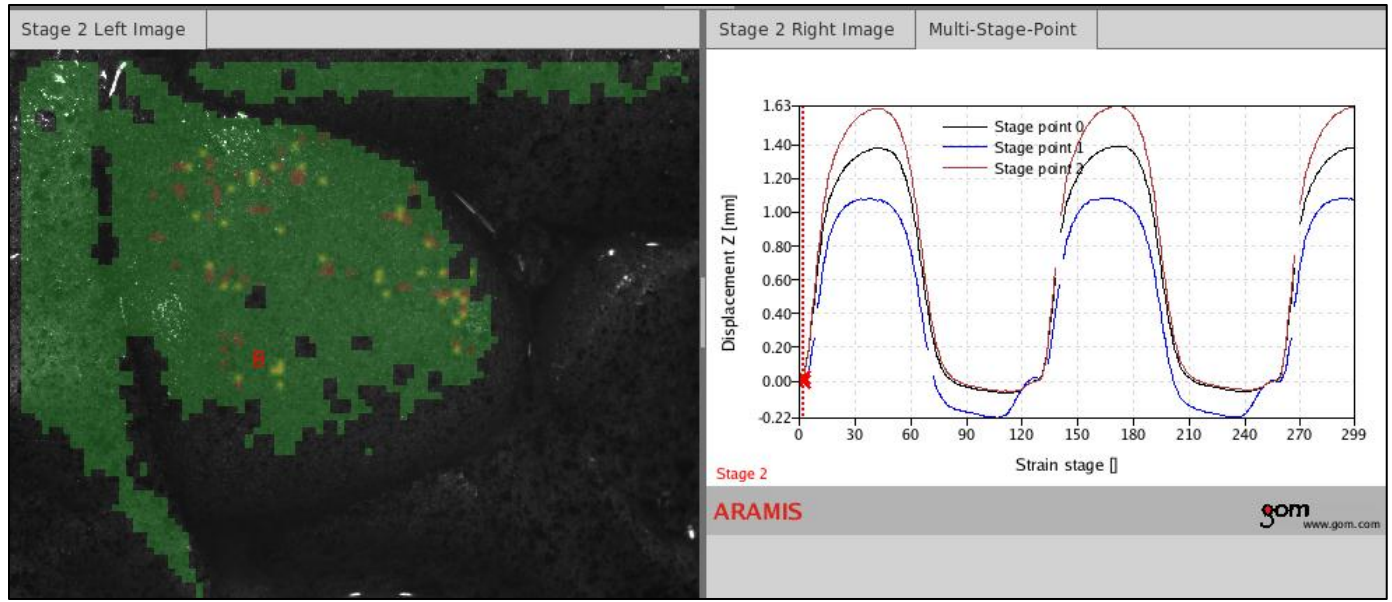


Figure 25: On the left is a stage image from the left camera showing the facet field over the heart surface. On the right is a plot of the displacements of three points.

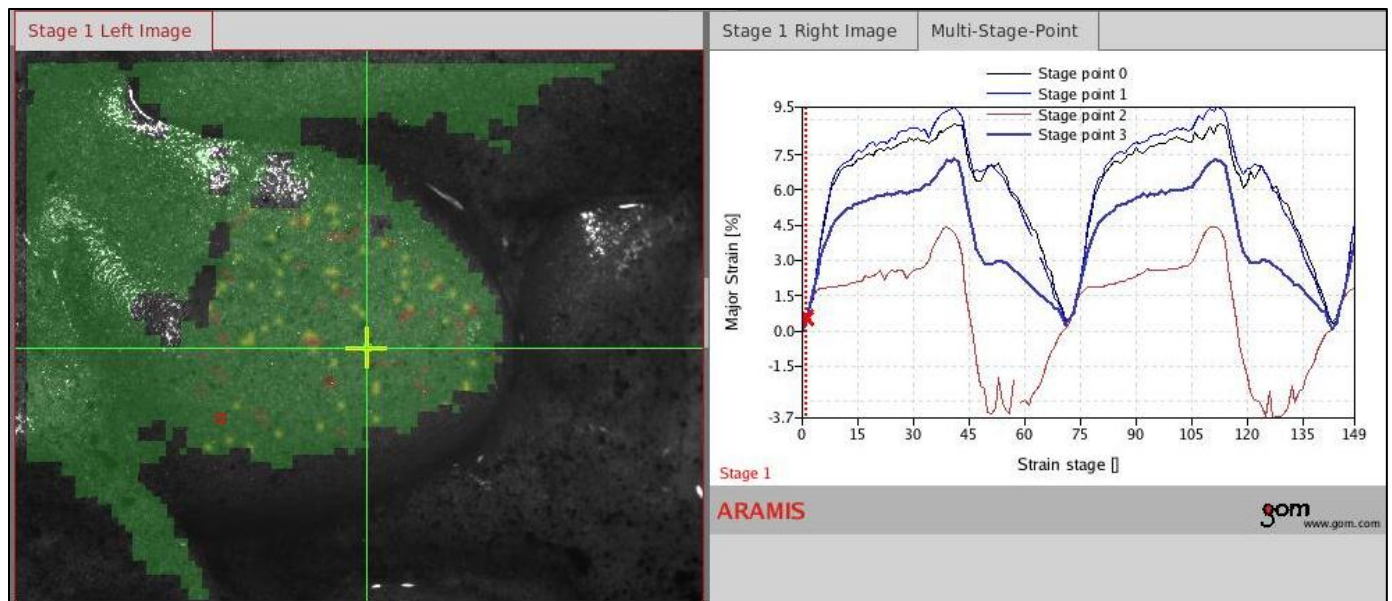


Figure 26: A strain plot for four points on the heart's ventricle (on the right). The plot is showing two heart beats in a period of three seconds.

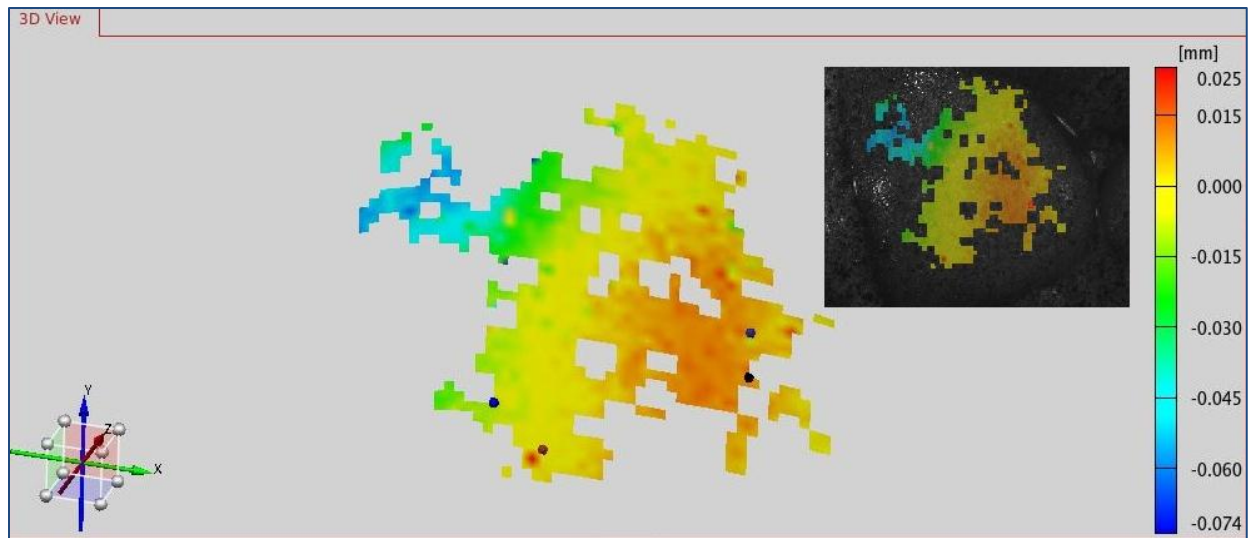


Figure 27: A 3D displacement image of the heart during a normotensive state. Insert is the displacement field on the heart to match view with exact location on heart surface.

Hypertensive Results

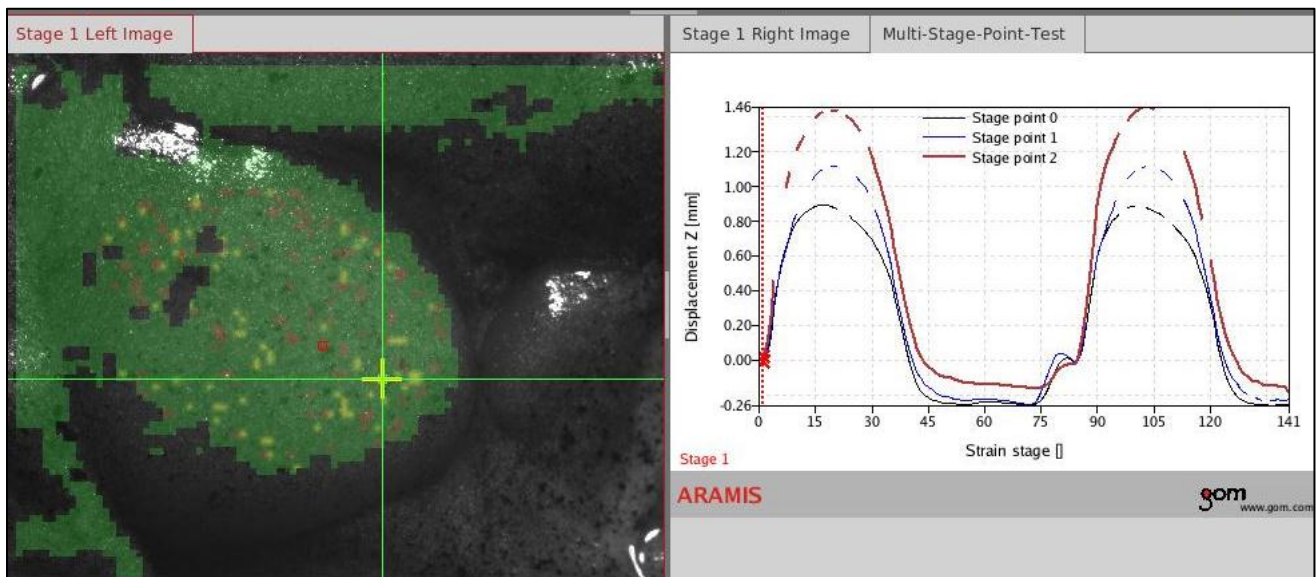


Figure 28: A facet field image on the left and a plot of the displacement on the right for selected points for a hypertensive state. The plots are still nicely synchronized even though the heart is hypertensive.

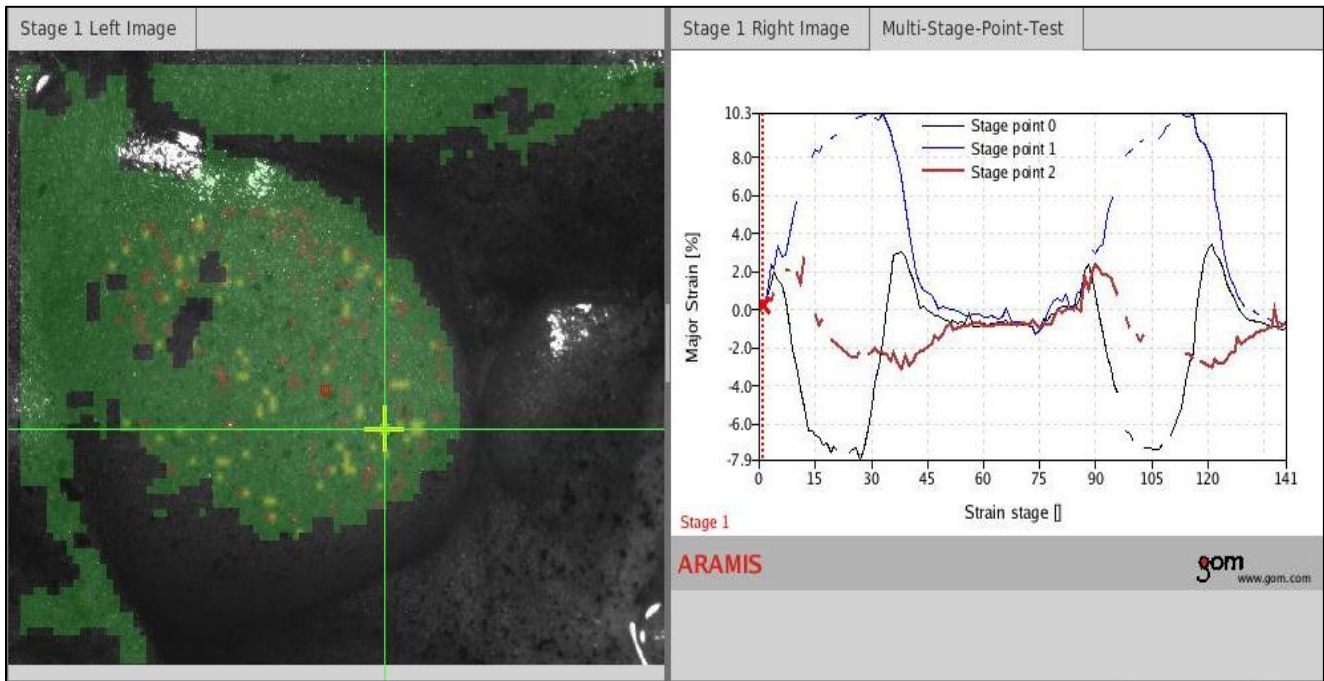


Figure 29: The strain results on the hypertensive heart (on the right) for selected facet points.

Several sets of data were collected for the normotensive state. Table 3 below summarizes the data. In both the displacement and strain columns, the range was calculated from each set, on the mostly deformed facet section, and then an average was calculated. The values in table 3 are the averages. For the hypertensive state, only one set of reliable data was obtained and used for comparison purposes.

Table 3: A comparison of the displacements and the strain on a normotensive state versus the hypertensive state.

	Displacement Z direction [mm]	Major Strain [%]
Normotensive State	1.45 ± 0.15	5.18 ± 1.9
Hypertensive State	1.63 ± 0.05	11.3 ± 0.5
Difference	0.177	6.12

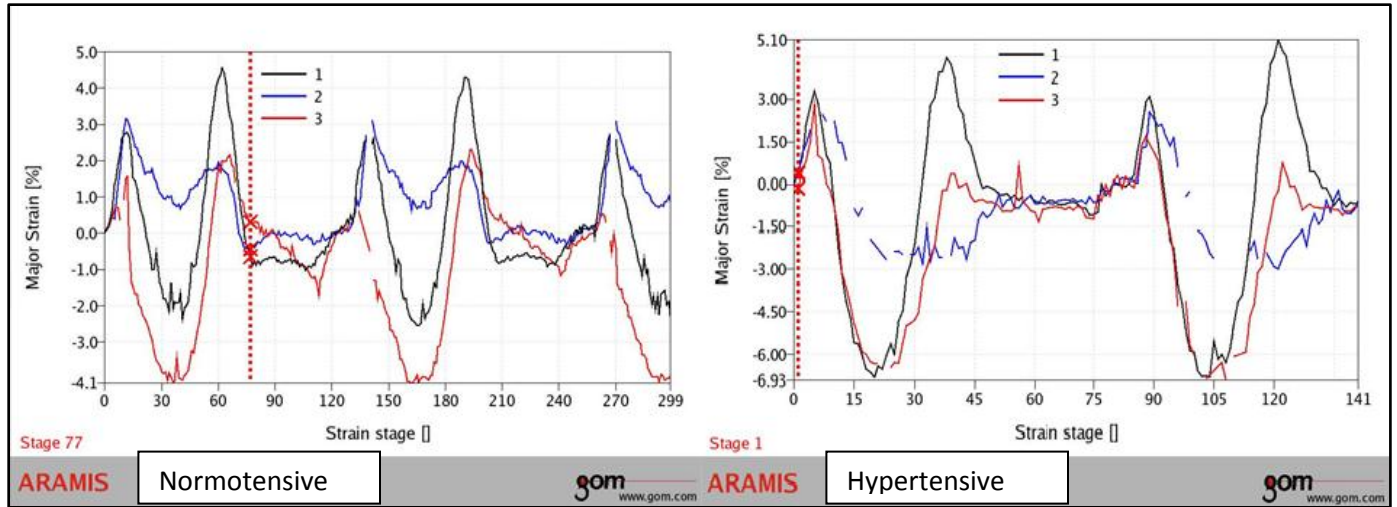


Figure 30: A strain comparison for same sections on ventricle, corresponding by numbers and colors. All three points seem to match in both states. Also notice that during hypertension, there is an increase in the range for each point. The two sets of data above were captured using 100 frames per second and 50 frames per second for the normotensive state and the hypertensive state respectively. They both span three seconds.

DISCUSSION

In this section the data presented in the results section and appendix D is discussed and evaluated. The goal is to assess how well the data supports or disagrees with the following hypotheses. 1) The contraction mechanism of the heart is a combination of the two models, that is, the peristaltic tube and the sphere chamber model. 2) During hypertension, the heart contracts more and beats are altered.

First, the validity of the data collected is checked. Initially, a pressure catheter transducer was to be connected to ensure that the heart beats normally. Unfortunately, it was not connected. A check on our data is then performed by comparing our data to past research. The results obtained match the data obtained by Adams when he measured the pressure inside the heart hence it is valid. These pressure measurements are shown in figure 31. More plots and figures are available in his report. (See reference 1)

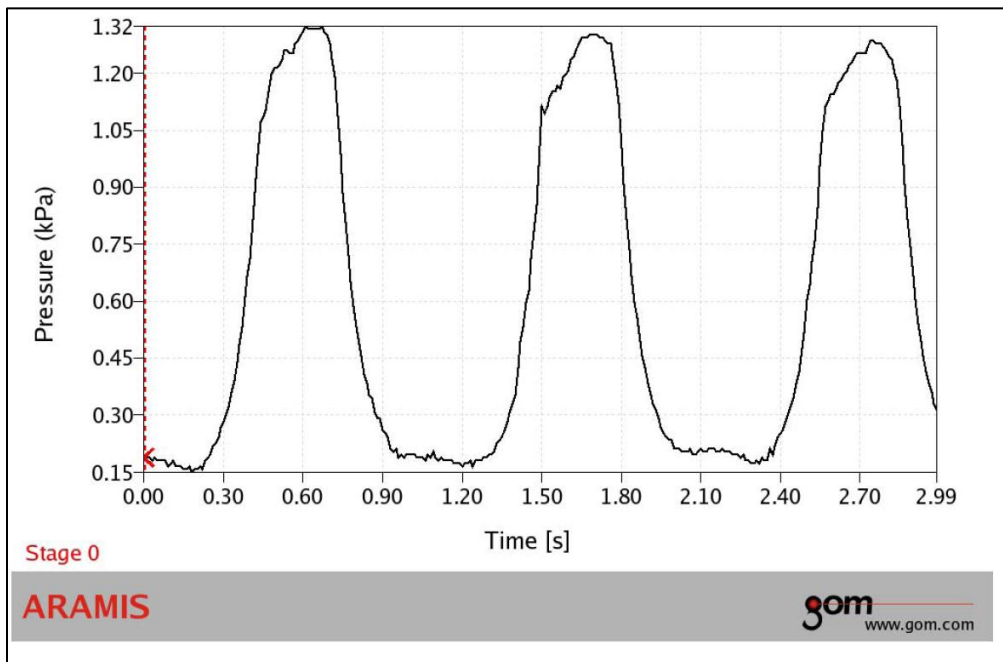


Figure 31: Ventricle pressure for a bull frog heart under a normotensive state. [1]

To determine the contraction mechanism of the heart, an analysis on the spatial displacements of the ventricle was performed. Based on the displacements plots in figures 25 and 28 it is tempting to conclude that the contraction mechanism is a sphere chamber model. Unfortunately, the data collected is not good enough to be used to make final conclusions. To augment this data, a set of data collected by Adams in 2009 for a normal beating heart was considered. Figure 32 below shows his plotted data for the Z displacements.

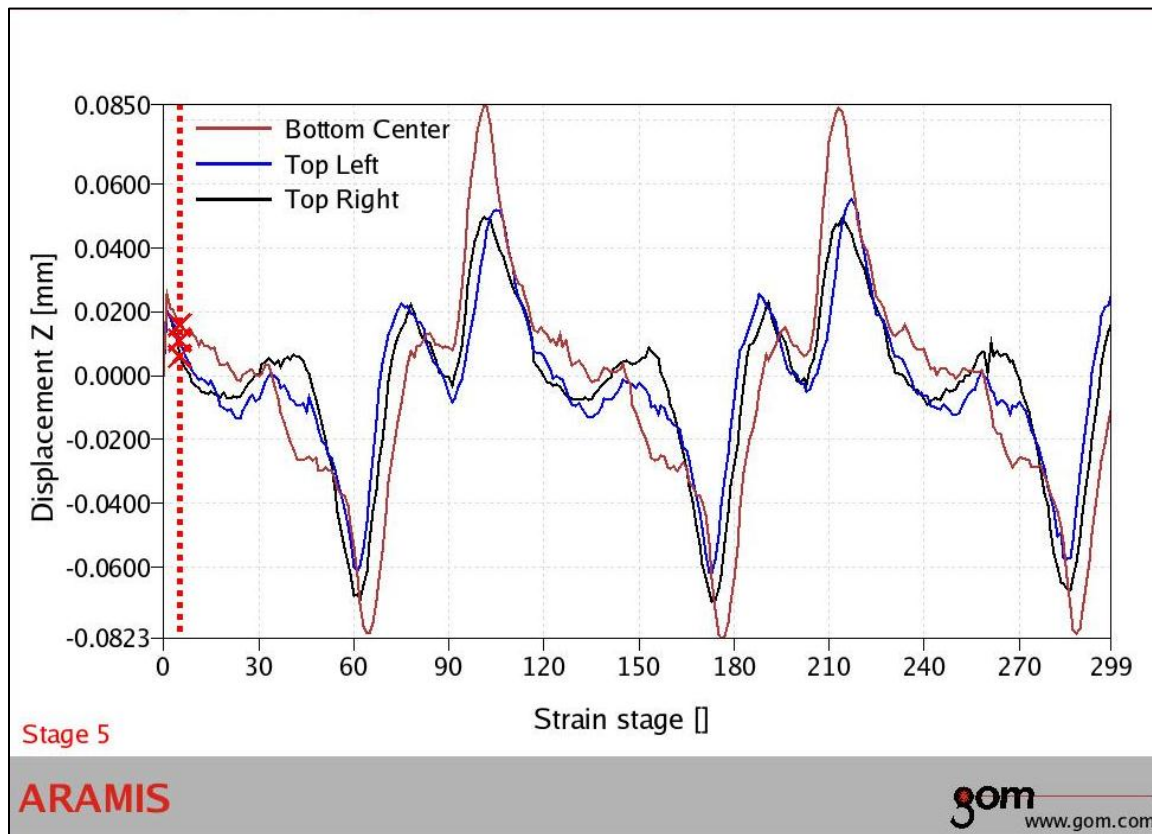


Figure 32: Displacements of a normal beating frog heart. [1] A larger view for this plot is attached in figure 41 in Appendix D. The three plots are synchronized with one another suggesting no time difference in the contractions of heart muscles..

In figure 32, the displacement plots have the same curve which supports the claim that the breathing mechanism of the heart is a sphere chamber model. The small misalignments can be attributed to experimental errors. The top left and right plots, blue and black respectively, are

smoothly synchronized – without a time shift. The plot for the displacements of the bottom center of heart is synchronized well with the other two. Figure 25 in the results section and figures 37 and 39 in Appendix D confirm the alignment of the displacement plots as for the data collected in this research. The ventricle, as seen in the images attached, is not a perfect sphere hence during the breathing process it appears that the center of contraction is outside the ventricle itself. Additionally, there are two exit passages for blood from the ventricle at the top; one to the lungs and the other to the rest of the body. The ventricle is basically ‘cone’ shaped with the top part connected to the two atria and the two exits. Its contraction mechanism matches a sphere chamber because its entire muscles contract at the same time and the data does not support the peristaltic tube model.

Based on the data obtained, it was concluded that deformations and strains of the heart increase from the ambient state to hypertension. Table 3 shows that the displacements increase by about 2 mm (0.177mm). This gives a percentage increase of 12 % from a normotensive state to a hypertensive state. The strains also increased from 5.18 % to 11.3 % showing a 6.1 % increase due to hypertension. It is important to note that only one set of data was taken during a hypertensive state. To reach any conclusions with respect to hypertension, a strain over the entire ventricle is required and more hypertensive data. Therefore, the second question for this research cannot be fully answered though the data seems to be in agreement with the hypothesis that hypertension increases the strains. Figure 30, for example, compares similar points in a normotensive state to a hypertensive state. Based on this graph the conclusion is that hypertension increases the strains but to quantify this increase, more than one hypertensive set of data is required. Additionally, figure 30 shows that during hypertension the heart beats are

slower than during the ambient state. Once again more data is required to quantify this time difference.

CONCLUSION

The most suitable contraction mechanism for the frog heart is the sphere chamber model. Hypertension increases the strains and deformations on the heart's ventricle as the heart 'struggles' to restore the ambient state. The data obtained was usable but not perfect. For instance figure 27, the 3D view of the displacement field of the heart, shows several facets unrecognized by the system resulting to the 'windows' in this view. Without a perfect displacement and strain field on the heart, not enough evidence is available to make accurate conclusions. However, the reports for specific facets displacement should be independent of the prior mentioned issue. Thus conclusions, in this document are based on the reports. Precisely, these are pre-conclusions.

RECOMMENDATION AND FUTURE WORK

The data collected under this research is rather insufficient for the author to make concrete conclusions. The experimental techniques were refined but not down to the required level of accuracy. The main issue presently is the speckling pattern. Developing this pattern is more of an art that requires care and commitment. A perfect speckling pattern is vital for the system to recognize all the facets in the heart's surface. In the future, more refinement for this technique is required to get useful data. Without deformation fields on the entire surface of the

ventricle, is it almost impossible to fully understand either the contraction mechanism or the ventricle's response to hypertension.

The lighting is a second priority issue. Notice that with the second and third experiments, halogen lights were added to the system. The polarized lights were not adequate for taking images at the required shutter time. During the first experiment it was noticed that taking images at 100 milliseconds results to blurry images. A recommended shutter time should be less than 20 milliseconds. Possibly using more fiber lights as opposed to the two currently in use would increase the lighting to the required level without introducing the glare in the images as is the case with the halogen lights.

Once the speckling and lighting issues have been solved, a pressure catheter transducer has to be connected to the heart to measure the pressure changes. In the summer of 2011, a smaller needle, 30G Mikro-tip, was acquired to reduce damages to the heart when inserting the needle tip into the ventricle. Due to time constraints and lack of success with the already mentioned issues, the catheter transducer was never connected to the heart. The pressure values will give information about the stress on the heart walls inside the ventricle and give more understanding of the contraction mechanism and response to hypertension of the heart. The techniques used for this research have been successful before hence the conviction that they can still be used to answer more research questions now and in the future.

REFERENCES

1. Adams, Matthew. "*In vivo* Measurements of Strain Field Gradients in an Amphibian Heart after artificially induced Myocardial Infarction." Union College. June 2009.
2. "Cardiovascular Diseases." World Health Organization. Retrieved: 7/25/2011.
<http://www.who.int/cardiovascular_diseases/en/>.
3. "Heart Disease and Stroke Statistics-2012 Update." *Circulation*. Web. 12 Mar. 2012.
<<http://circ.ahajournals.org/content/125/1/e88>>.
4. "High Blood Pressure: MedlinePlus." *U.S National Library of Medicine*. U.S. National Library of Medicine. Web. 12 Mar. 2012.
<<http://www.nlm.nih.gov/medlineplus/highbloodpressure.html>>.
5. Pepe, Leah. "An analysis of hypertension and its relation to spacio-temporal contractions of the amphibian heart." Union College. June 2011.
6. Robinson, Scott. "The Photogrammetry of Bullfrog Hearts.' Union College. 2003.
7. Goodman, Amanda. "The Photogrammetry of Bullfrog Hearts. Retrieved 2/8/11.
<http://www.union.edu/academic_depts/mechanical_eng/students/projects/06/Goodman.pdf>
8. Guernon, Alexandra and Adams, Matt. "The Photogrammetry of Bullfrog Hearts." Retrieved 2/8/11.
<<http://www.union.edu/academic_depts/mechanical_eng/students/projects/Summer08/Guernon_Alex_S08.pdf>>
9. "NIH Fact Sheets - Hypertension (High Blood Pressure)." *NIH Research Portfolio Online Reporting Tools (RePORT)*. Web. 13 Mar. 2012.
<<http://report.nih.gov/NIHfactsheets/ViewFactSheet.aspx?csid=97>>

10. Lazaroff. "Bullfrog Dissection." *Bullfrog Dissection*. Web. 29 Feb. 2012.
<<http://shs.westport.k12.ct.us/mjvl/biology/dissect/frog.htm>>.
11. Randall David, Warren Burggren and Kathleen French. *Animal Physiology: Mechanics and Adaptations*. 4th. New York: W.H. Freeman and Company, 1997.
12. Interactive Biology. "The human Heart." Accessed 9/29/2011. <<http://www.interactive-biology.com/wp-content/uploads/2009/12/heart.png>>
13. Field J., Walley S., Proud W., Goldrein H. and Siviour C. *International Journal of Impact Engineering* 30 (2004) 725–775. "Review of experimental techniques for high rate deformation and shock studies". Accessed 10/12/2011.
<<http://www.smf.phy.cam.ac.uk/Publications/Strength%20papers/576StrFieldIJIE30.pdf>>
14. "Millar Instruments" Research Products. Accessed 5/27/2011.
<<http://millar.com/products/research>>
15. Çengel, Yunus A., and John M. Cimbala. *Fluid Mechanics: Fundamentals and Applications*. Boston: McGraw-Hill Higher Education, 2006. Print.
16. Gom. "ARAMIS v6 User Manual – Software." Braunschweig, Germany: 2007.
17. "The Circulation of the Human Body." Retrieved 2/8/2011
18. "Profile: Cane Toad (Bufo Marinus)." *Off Beat Pets*. Web. 12 Mar. 2012.
<<http://www.offbeatpets.com/amphibians/profile-cane-toad-bufo-marinus/>>.
19. "The Biology Corner." *The Biology Corner*. Web. 12 Mar. 2012.
<<http://www.biologycorner.com/myimages/frog-dissection/>>.

APPENDIX

APPENDIX A: ARAMIS Calibration Data

Table 4: Calibration table for ARAMIS Photogrammetry System. (b) is an extension for (a) with a focus on the 12 x 15 mm cube which is mainly used to calibrate the system for heart experiments.

(a)

For polarized lights	Calibration Cube			
	8x10	12x15	20x25	28x35
Lens/Focal Length	50 mm	50 mm	50 mm	50 mm
Filters	yes	yes	yes	yes
Type of Light	polarized	polarized	polarized	polarized
Extensions	40 mm	35 mm	20 mm	15 mm
Distance between cameras	140 mm	130 mm	130 mm	140 mm
Distance from target	170 mm	180 mm	225 mm	255 mm
Camera Angle (°)	40	34	31	30

(b)

12x15 mm Cube	Distance between cameras (mm)			
	120	130	130	140
Lens/Focal Length	50 mm	50 mm	50 mm	50 mm
Filters	yes	yes	yes	yes
Type of Light	polarized	polarized	polarized	polarized
Extensions	35 mm	35 mm	40 mm	35 mm
Distance from target	182 mm	180 mm	178 mm	174 mm
Camera Angle (°)	34.9	36.9	37.9	40?
Cal Deviation (pixels)	0.052	0.048	0.083	0.241
Measuring Volume	20x15x5 mm	20x20x10 mm	20x15x5 mm	20x15x5 mm

Appendix B: Lights Holder Piece

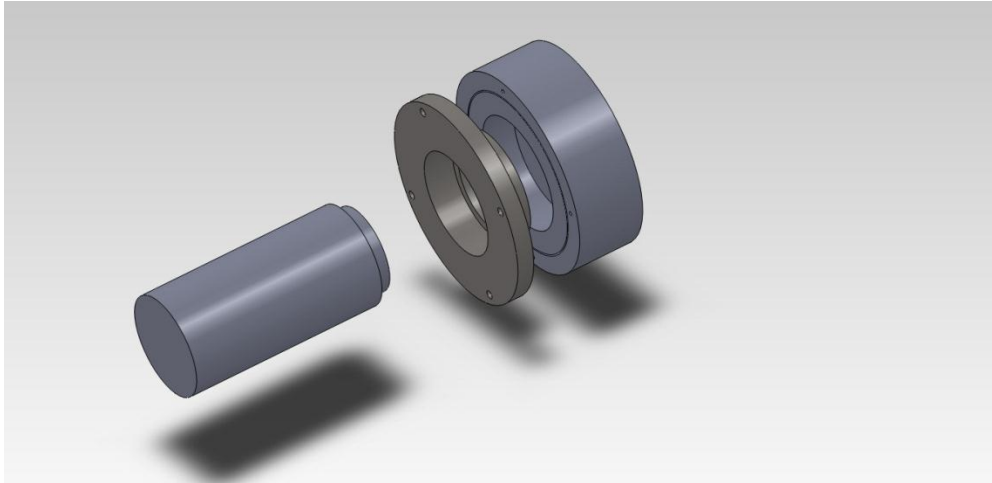


Figure 33: The designed piece (in between) used to securely connect filters at the end of the light's projecting arms.

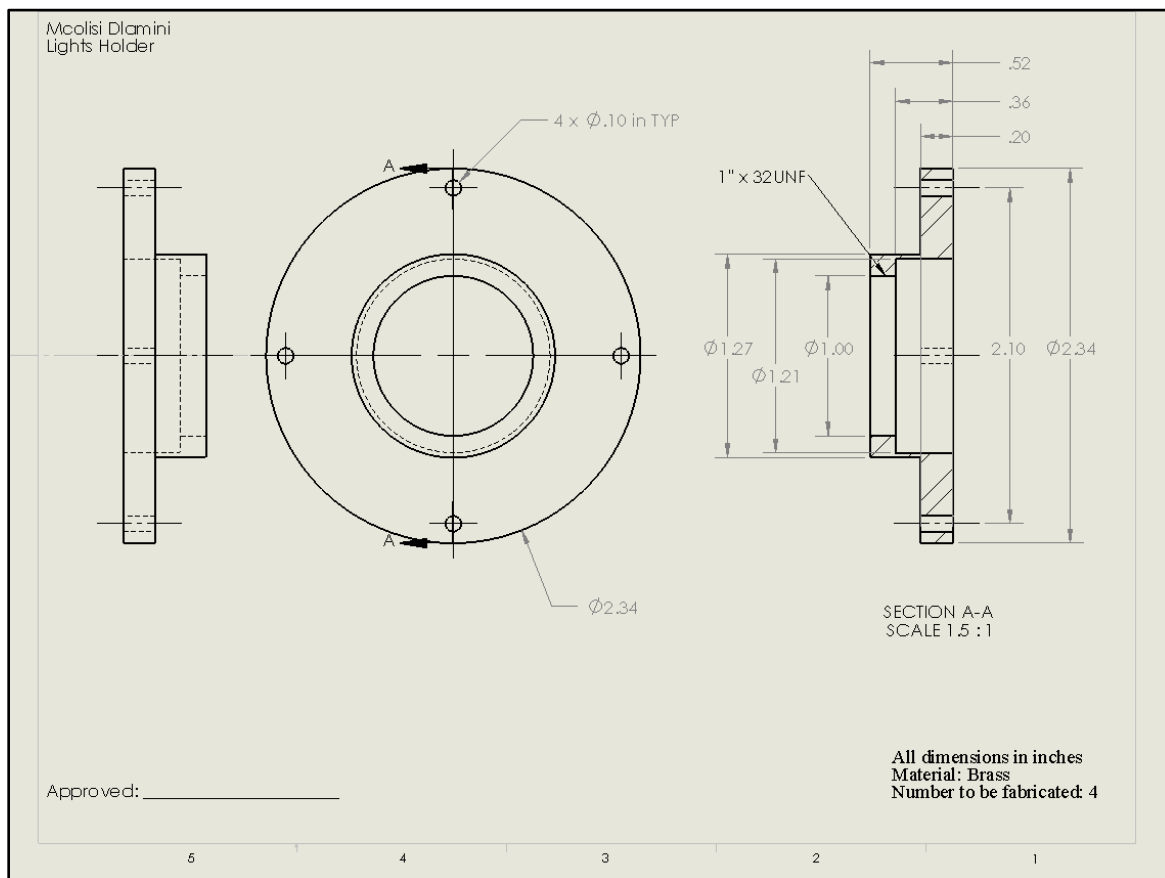


Figure 34: A drawing of the brass piece that is shown in the figure above.

APPENDIX C: Pressure Transducer and Catheter Transducer Calibration

Table 5: Data and calculations for the case without a needle.

Without Needle							
Water Level (mL)	Depth (mm)	Δh (mm)	Voltage Output (mV)		Pressure (Pa)	Pressure change	
			Average	Difference	$\rho g \cdot \text{depth}$	$\rho g \cdot \Delta h$	Pressure per volt
450	27.5	27.5	34.60		270	270	
400	55	27.5	54.63	20.03	540	270	13466
350	82.5	27.5	72.70	18.07	809	270	14932
300	110	27.5	92.33	19.63	1079	270	13741
250	138	28	112.50	20.17	1354	275	13620
200	165.8	27.8	131.77	19.27	1626	273	14155
150	193.5	27.7	153.17	21.40	1898	272	12698
Average =>		27.64		19.76		271.41	13768.76
StDev =>		0.20		1.10		2.03	743.44

Table 6: Data used to calibrate the 30 G hypodermic needle.

30 gauge needle							
Water Level (mL)	Depth (mm)	Δh (mm)	Voltage Output (V)		Pressure (Pa)	Pressure change	
			Average	Difference	$\rho g \cdot \text{depth}$	$\rho g \cdot \Delta h$	Pressure per volt
450	27.5	27.5	14.40		270	270	
400	55	27.5	17.80	3.40	540	270	79346
350	82.5	27.5	40.40	22.60	809	270	11937
300	110	27.5	60.47	20.07	1079	270	13444
250	138	28	80.63	20.17	1354	275	13620
200	165.8	27.8	99.80	19.17	1626	273	14229
150	193.5	27.7	120.10	20.30	1898	272	13386
Average		27.64		19.93		271.41	13669.81
STDEV		0.20		1.28		2.03	385.74

Table 7: Data used to calibrate the 19 G needle.

19 gauge Needle							
Water Level (mL)	Depth (mm)	Δh (mm)	Voltage Output (V)		Pressure (Pa)	Pressure change	
			Average	Difference	$\rho g * \text{depth}$	$\rho g * \Delta h$	Pressure per volt
450	27.5	27.5	19.20		270	270	
400	55	27.5	20.10	0.90	540	270	299750
350	82.5	27.5	30.90	10.80	809	270	24979
300	110	27.5	50.33	19.43	1079	270	13882
250	138	28	71.87	21.53	1354	275	12756
200	165.8	27.8	91.03	19.17	1626	273	14229
150	193.5	27.7	110.47	19.43	1898	272	13983
	Average	27.64		19.89		271.41	13712.48
	STDEV	0.20		1.10		2.03	654.04

Table 8: A summary of calibration data for all the two needles tested. This data was used to generate figure 16.

Water Level (mL)	Height (mm)	Voltage Output (mV)			Pressure (Pa)
		Without Needle	30 G	19 G	
450	27.5	34.6	14.4	19.2	269.8
400	55	54.6	17.8	20.1	539.6
350	82.5	72.7	40.4	30.9	809.3
300	110	92.3	60.5	50.3	1079.1
250	138	112.5	80.6	71.9	1353.8
200	165.8	131.8	99.8	91.0	1626.5
150	193.5	153.2	120.1	110.5	1898.2

Appendix D: Results

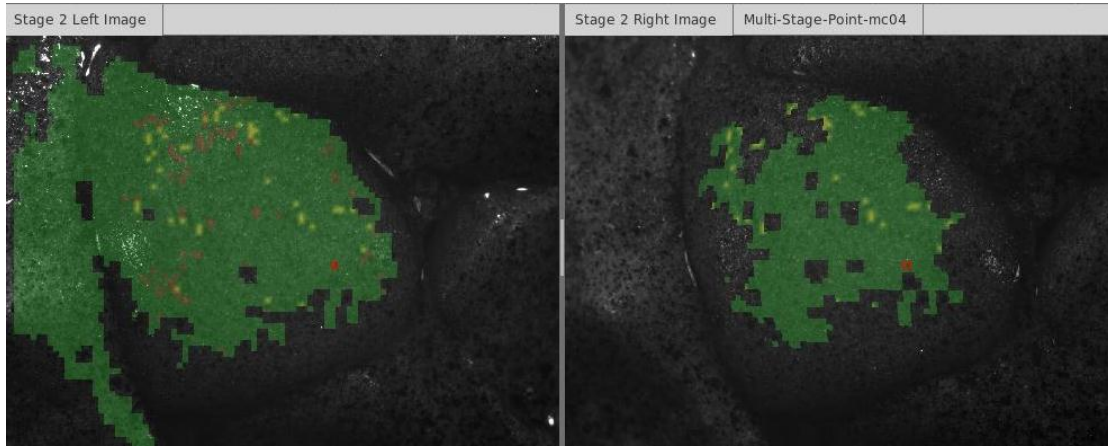


Figure 35: The left and right images with facet fields. The image on the right shows much less facets suggesting a correlation issue in the system. *[Normotensive State]*

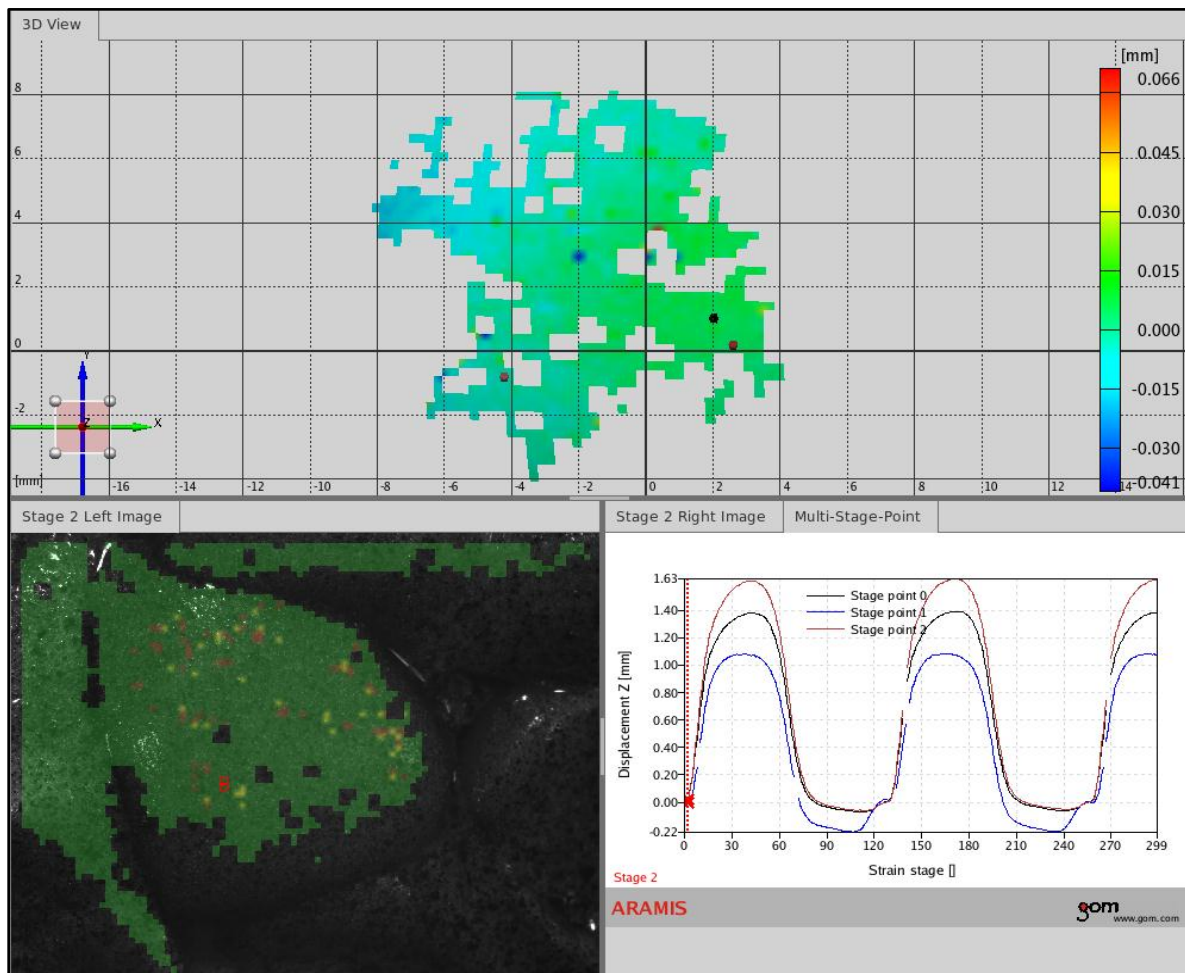


Figure 36: An image showing the left image, the report and the 3D view of the displacement field. *[Normotensive State]*

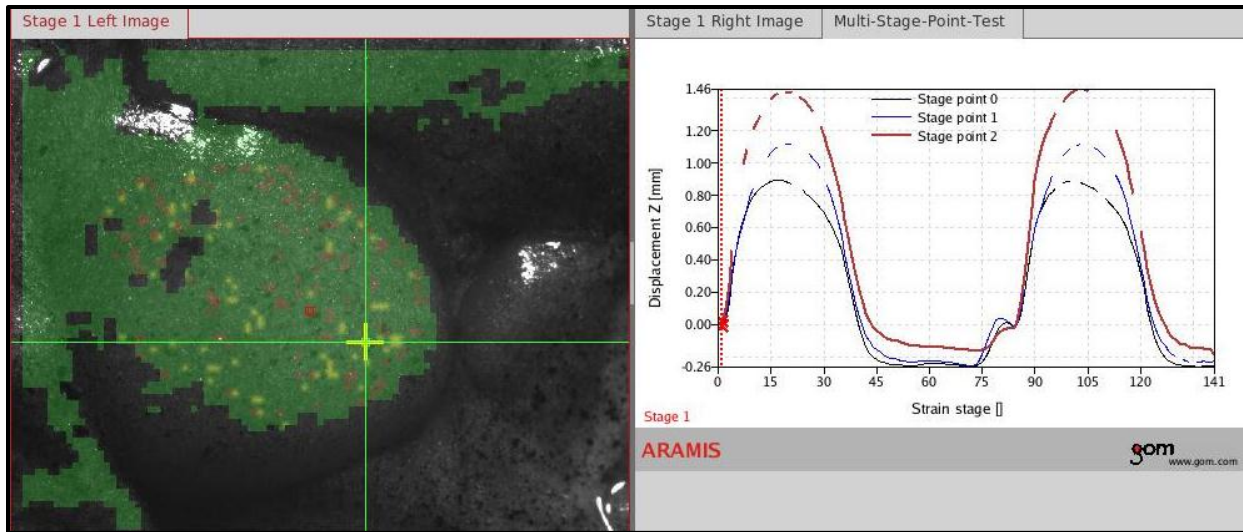


Figure 37: On the left is an image of the heart with facet fields. On the right is plot of the displacements for three selected points on the ventricle. *[Normotensive State]*

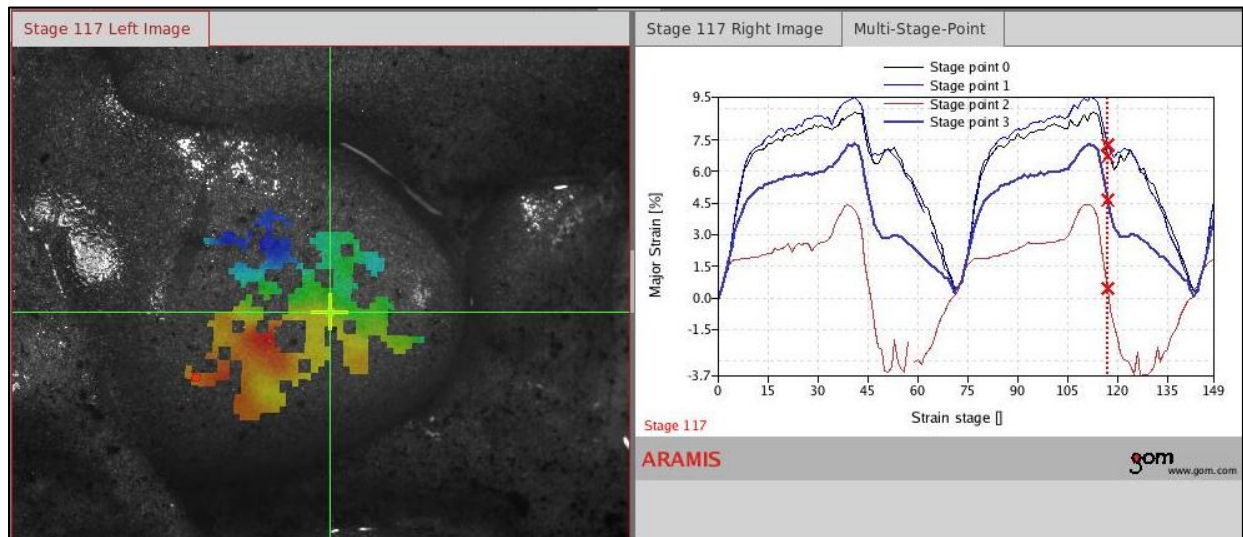


Figure 38: This figure shows the strains on a normotensive heart. On the left is the strain field and on the right is a plot of the strain for four selected points on the ventricle. *[Normotensive State]*

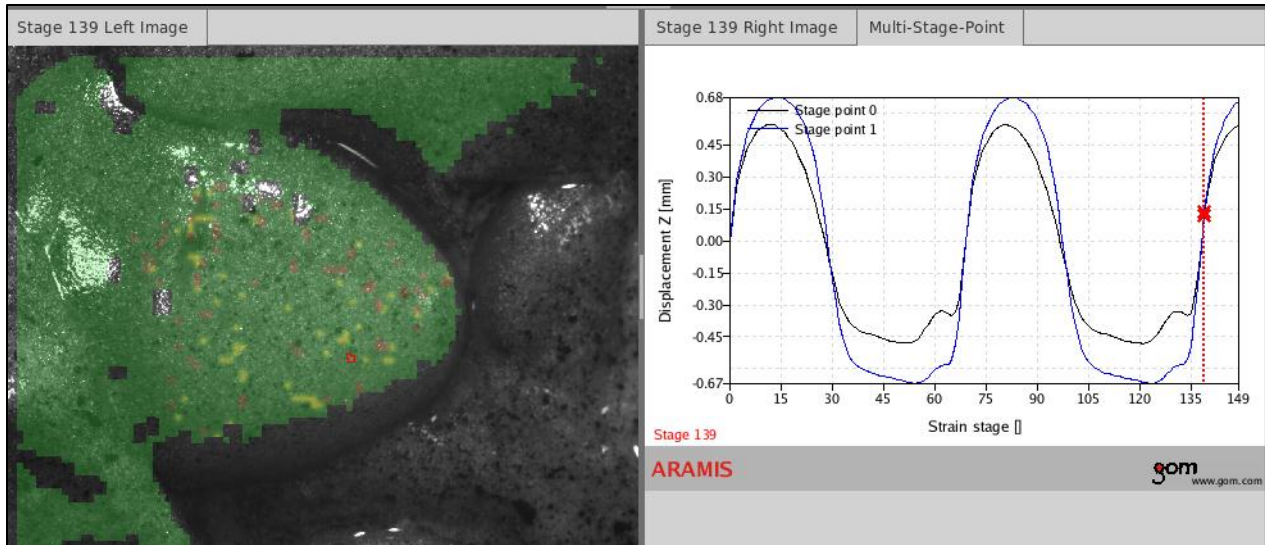


Figure 39: Top left is the facet field and on the right is a graph showing the displacements of point 0 on the top side of ventricle and stage point 1 on the lower side of ventricle.
[Normotensive State]

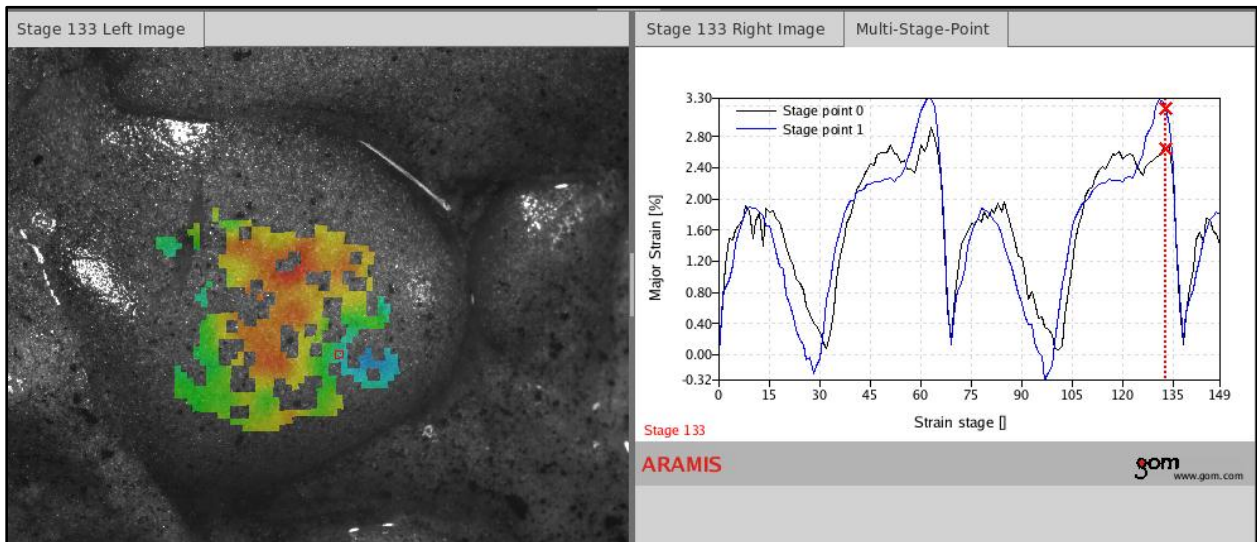


Figure 40: On the left is strain field on the heart not covering entire surface of the heart due to poor speckling. On the right is a strain plot for stage point 0 and stage point 1, on the ventricle.
[Normotensive State]

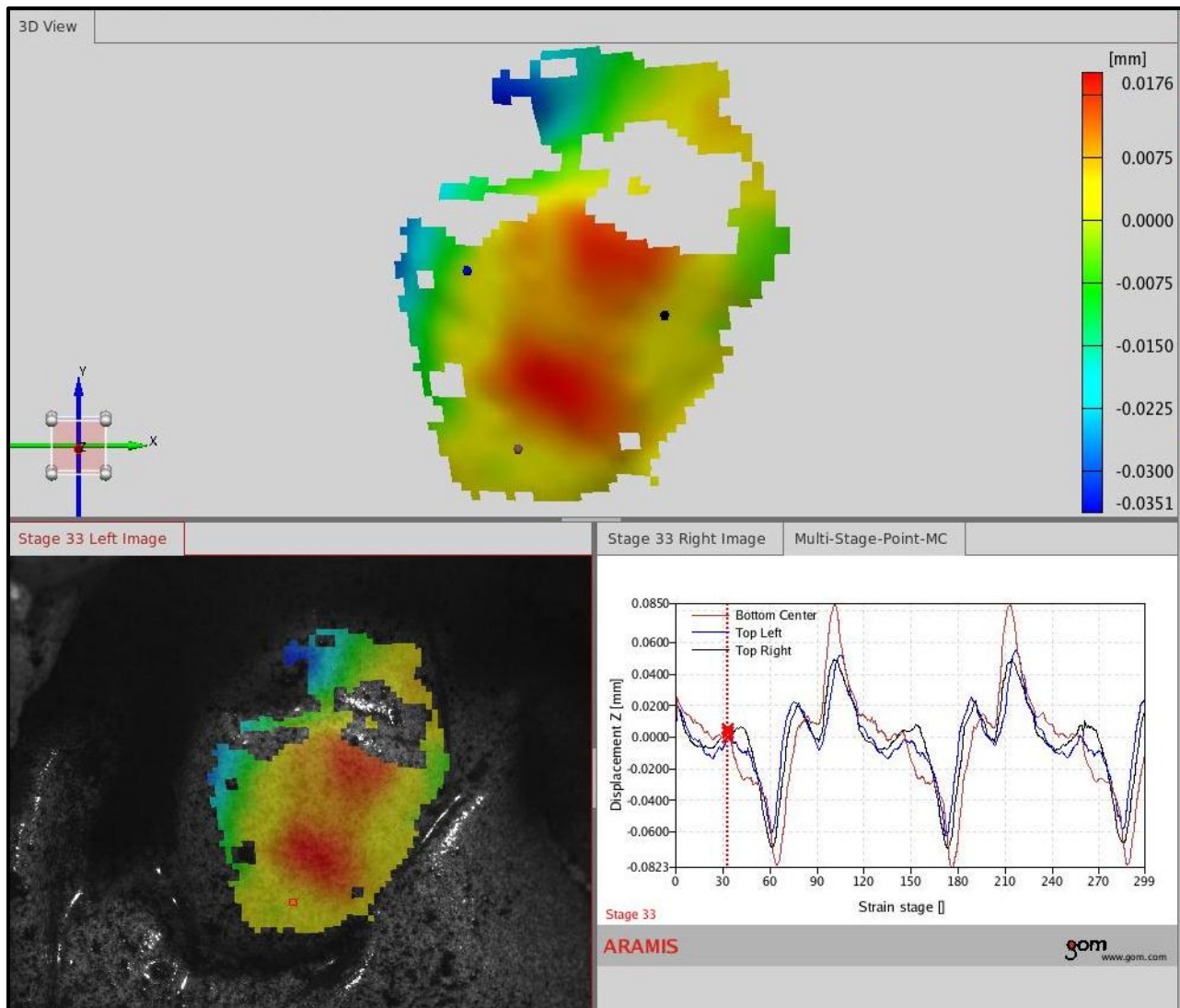


Figure 41: The displacement field for a normotensive state. Above is a 3D view of the displacement field. Below left is the heart and strain fields on it, and bottom right is a plot of the displacements for a set of data. This data was collected by Adams in 2009. [1] *[Normotensive State]*